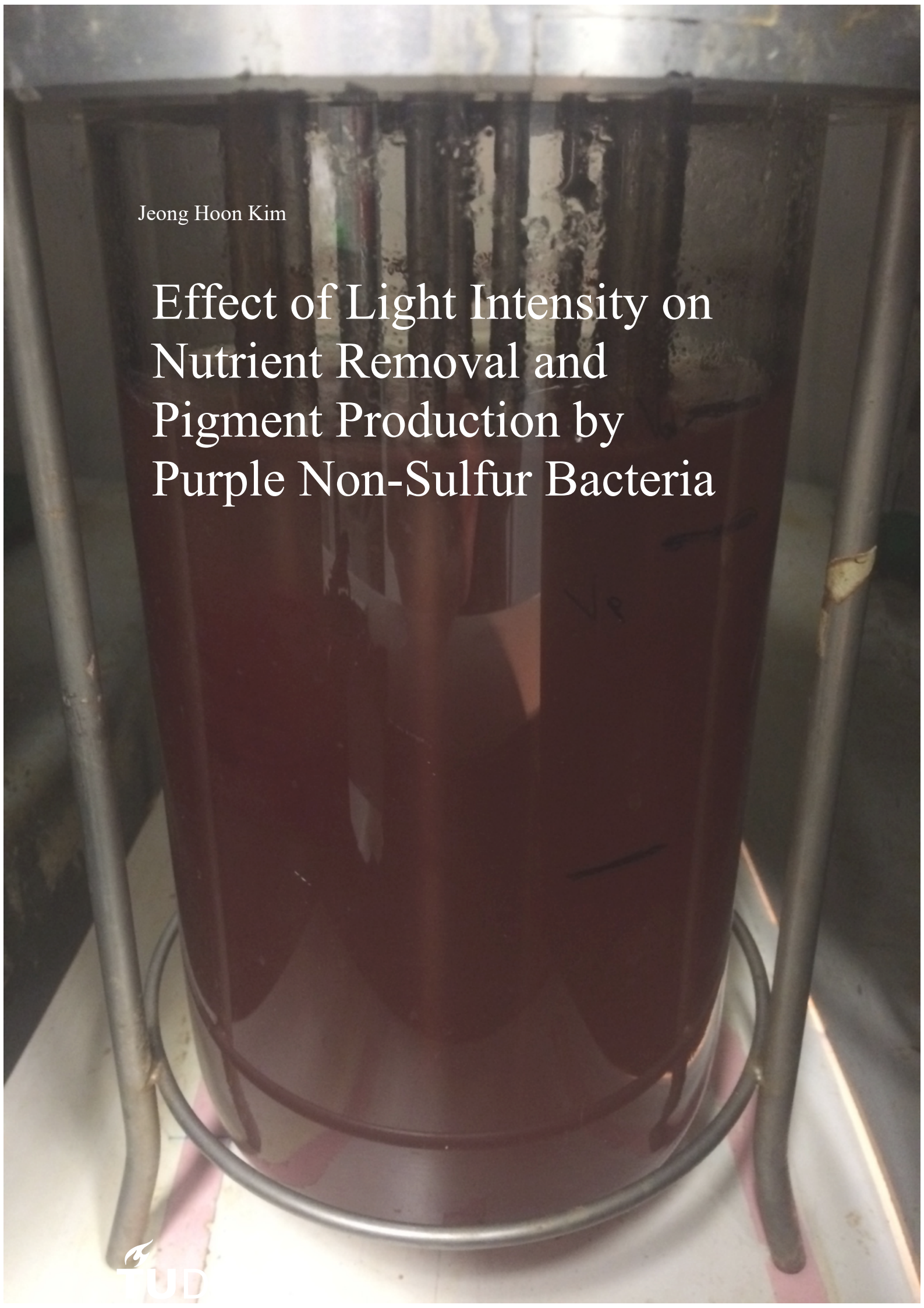

Jeong Hoon Kim

Effect of Light Intensity on Nutrient Removal and Pigment Production by Purple Non-Sulfur Bacteria

Effect of Light Intensity on Nutrient Removal and Pigment Production by Purple Non-Sulfur Bacteria

By

Jeong Hoon Kim

in partial fulfilment of the requirements for the degree of

Master of Science

in Civil Engineering and Geosciences

at the Delft University of Technology,

This MSc thesis was conducted at the:

Weissbrodt Research Group for Environmental Life Science Engineering
Environmental Biotechnology Section, Department of Biotechnology, Faculty of Applied Sciences
Delft University of Technology
van der Maasweg 9, 2629 HZ Delft, The Netherlands

Correspondence: J.H.Kim-3@student.tudelft.nl ; M.Cerruti@tudelft.nl ; D.G.Weissbrodt@tudelft.nl

Thesis advisor:	David Weissbrodt, Assistant Professor
	Marta Cerruti, PhD candidate
Thesis committee:	Ralph Lindeboom, Assistant Professor
	Merle de Kreuk, Full Professor
	Sirous Ebrahimi, Visiting Full Professor

This thesis is confidential and cannot be made public until new notice by David Weissbrodt, thesis director.

Contents

TU Delft

Glossary

Notation	Definition	Units
I	Light intensity obtained at distance 'x'	W m^{-2}
$I_{0,\lambda}$	Spectral irradiance of incident light	W m^{-2} nm^{-1}
I_0	Incident light intensity	W m^{-2}
I_{avg}	Average light intensity obtained in the reactor	W m^{-2}
I_λ	Spectral irradiance obtained at distance 'x'	W m^{-2} nm^{-1}
$K_{S_{ac}}$	Half velocity constant of acetate	mg L^{-1}
$K_{S_{am}}$	Half velocity constant of ammonium	mg L^{-1}
K_{S_I}	Half velocity constant of light intensity	W m^{-2}
$K_{S_{PO}}$	Half velocity constant of phosphate	mg L^{-1}
L	Distance from light source to reactor	m
R	Photo-bioreactor radius	m
S_{ac}	Acetate concentration	mg L^{-1}
S_{am}	Ammonium concentration	mg L^{-1}
S_I	Average light intensity	W m^{-2}
S_{PO}	Phosphate concentration	mg L^{-1}
x	Distance from reactor surface	m
X_p	PNSB Biomass concentration	mg L^{-1}
$Y_{X/S_{ac}}$	Biomass yield on acetate	mg mg^{-1}
$Y_{X/S_{am}}$	Biomass yield on ammonium	mg mg^{-1}
$Y_{X/S_{PO}}$	Biomass yield on phosphate	mg mg^{-1}
$\varepsilon_{cell,\lambda}$	Spectral mass attenuation coefficient of cell	m^2 g^{-1} nm^{-1}
ε_{cell}	Mass attenuation coefficient of cell	m^2 g^{-1}
μ_{max}	Maximum biomass specific growth rate	h^{-1}

List of Figures

List of Tables

Graphical abstract

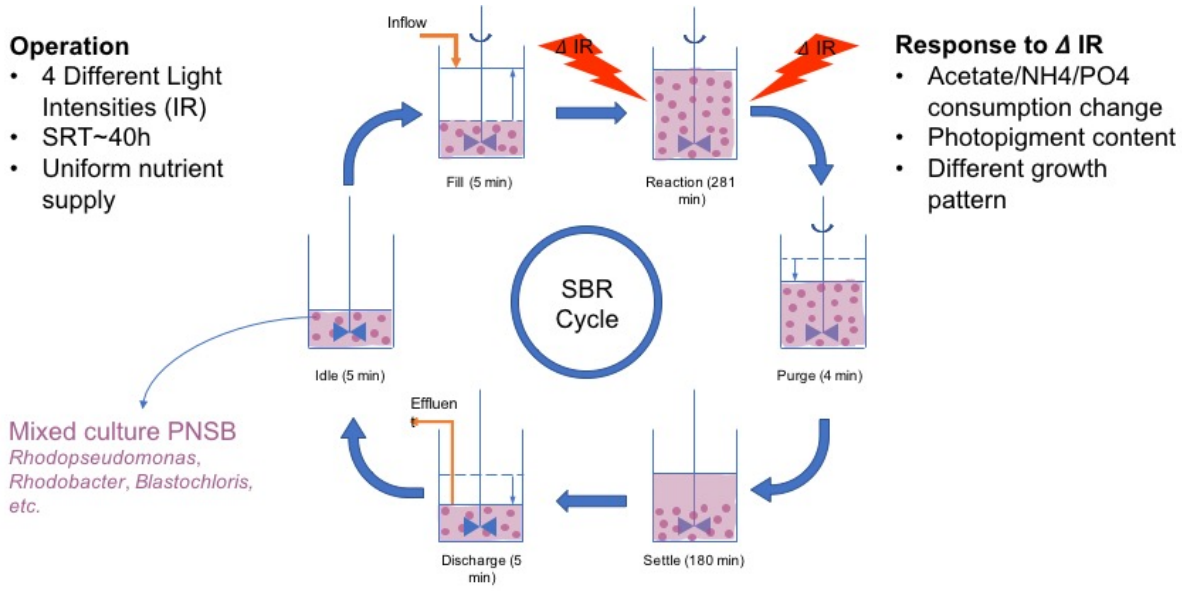

Abstract

Purple non-sulfur bacteria (PNSB) consist of wide genera of phototrophic bacteria found in various aquatic system. A high versatility in their mode of growth ranging from photoheterotrophic to dark fermentation gives them various potential applications. Their nature of being phototrophs require them to obtain light as energy source for growth and for that they require photopigments essential for light to ATP conversion. In contrast to pure culture of PNSB, the effect of different illumination on mixed culture PNSB is partly revealed. The response of altering light intensity on mixed culture of PNSB and the change of photopigments were to be answered in this study. Mixed culture of PNSB were grown in a sequencing batch reactor (SBR) operation of 8 h cycle. Four different light intensity settings were used to identify the effect of light on their growth and nutrient removal rate. Light distribution model was constructed to simulate the growth and nutrient removal of pure culture *Rhodopseudomonas palustris* in order to compare with mixed culture PNSB results. To track the growth and nutrient removal trend, biomass and nutrients (acetate, ammonium, and phosphate) concentrations at different points during reaction phase were measured. Bacteriochlorphyll content as major photopigment was analyzed with two different methods; micro well plate reader and reverse-phased HPLC. It was shown that both growth rate and nutrient removal rate were significantly diminished as light intensity decreased. Growth rate has decreased to 82% (75% light intensity), 36% (50% light intensity), and 19% (25% light intensity) of its original rate at baseline intensity (100%, 350 W m^{-2}). The decrease of growth rate with decreasing light intensity indicated that with the given conditions, light intensity was the growth rate-limiting factor for the mixed culture PNSB studied. In comparison to simulation results, it was shown that the mixed culture PNSB was showing faster growth and higher removal rate. Bacteriochlorophyll content in the micro plate reader showed an increase to 75% intensity condition and then a decrease to 25% intensity conditions. Bacteriochlrophyll content analyzed by the two different methods showed relatively high deviation between each other as large error in both analyzing methods were present. The effect of changing light intensity on mixed culture PNSB with respect to its growth, nutrient removal and pigment content was studied. Further investigation on both higher and lower light intensity to identify the photo-inhibition level and saturation level is necessary. For a better approximation of the simulation to experimental data, further works on precise measurement of light distribution in the photobioreactor is required. Photo-pigment analysis methods should be either replaced by a spectrophotometer using standardized cuvettes to minimize measurement error or be optimized to obtain reliable data.

Acknowledgements

First of all, I would like to show my deepest gratitude to both my supervisors David Weissbrodt and Marta Cerruti for their precious scientific input and support for the past 8 months of work. It has been an invaluable time of learning how to approach a scientific question, organize works, and to critically think. The time I have spent working with them have been a great experience and a chance to improve myself in both personal character and ability wise.

Secondly, I would like to thank my thesis committee members Merle de Kreuk, Ralph Lindeboom, and Sirous Ebrahimi for their kind support and excellent input in my thesis. I would also like to thank the staff members Rob Kerste, Dirk Geerts, Cor Ras, Rhody Breukman, and Ben Abbas for their technical support and input. I would also like to thank my everyone in the EBT section for their warm welcome.

Finally, I would like to thank my parents and friends for their enormous support and encouragement. This achievement would have never been made without their unconditional support and love.

This study was funded by the start-up grant of Department of Biotechnology, TU Delft.

1. Introduction

1.1. Background

1.1.1. What are Purple Non-sulfur Bacteria?

Purple nonsulfur bacteria (PNSB) form a wide guild of photosynthetic microorganisms spanning over different classes and genera (Madigan & Jung, 2009). In early works, PNSB have been believed to not grow in environment where sulfide was present in contrast to purple sulfur bacteria (PSB) which can grow in such condition and oxidize sulfide (van Niel, 1944). However, Hansen and van Gemerden (1972) have shown that such distinction was not valid as PNSB can grow and oxidize sulfide at low concentration of sulfide. Instead of distinguishing them by the tolerance and utilization of sulfide, they are distinguished by the fate of formed elemental sulfur in their cell; PNSB deposit formed sulfur outside their cell whereas PSB stores it intracellularly as globules (Brune, 1995; Hansen & van Gemerden, 1972).

Growth of some PNSB, *e.g. Rhodobacter capsulatus,* is possible under phototrophic conditions with either CO_2 or organic carbon, or in darkness by respiration, fermentation, or chemolithotropy (Vinet & Zhedanov, 2011). Among the capable modes of growth, photoheterotrophic growth is the best mode of growth for PNSB (Sojka, 1978). Nonetheless, no known PNSB is capable of hydrolyzing complex polymeric organic substances like starch or cellulose and thus, they primarily rely on other heterotrophs to degrade those complex substances into simpler compounds available for consumption (Pfennig, 1978). Because of their versatile metabolism, PNSB can be found in geographical locations where light is present and sulfide concentration is low. Sewage (Siefert, Irgens, & Pfennig, 1978) or waste lagoons (Cooper, Rands, & Woo, 1975) are typical aquatic system populated by PNSB.

From the versatility of PNSB arise numerous possible applications. In the absence of ammonium, PNSB can produce bio-hydrogen – a central product of their metabolism – which can be utilized in hydrogen fuel cells. This aspect has been extensively studied axenic bioprocesses (Adessi & De Philippis, 2014; Akkerman, Janssen, Rocha, & Wijffels, 2002; Androga, Özgür, Eroglu, Gündüz, & Yücel, 2012; Levin, Pitt, & Love, 2004). Another biotechnological application of PNSB utilization links to the production of useful cell materials like proteins and enzymes. Their versatility further provides a definite advantage to convert various organic substrates (e.g. soybean curd, aromatic compounds) from diverse aqueous waste streams such as municipal and industrial wastewater, and green waste hydrolysates

(Harwood & Gibson, 1988; Hiraishi, Shi, & Kitamura, 1989; Hülsen, Batstone, & Keller, 2014).

Here, the photoheterotrophic mode of growth was under focus, since the aim of this study was to investigate the light intensity effect on growth and nutrient removal, and pigment production of a PNSB mixed culture bioprocess fed with synthetic domestic wastewater. Under photoheterotrophic growth, PNSB absorb light using a special complex in their cell membrane (this part will be further explained in the next section), convert this light energy into chemical energy in the form of ATP via their membrane protein complexes, and use ATP for growth and cell maintenance. Since they do not utilize carbon substances as energy source, unlike ordinary heterotrophs, the carbon substances they uptake can be almost fully utilized for building up cell materials in their metabolism (Madigan & Jung, 2009). This characteristic of photoheterotrophic growth is the reason why they have much higher growth yield on substrates than any other mode of growth among ordinary heterotrophs. For instance, biomass yield of *Rhodopseudomonas sphaeroides* S in photoheterotrophic growth ranges from 5.0 to 5.8 g cell/ave whereas aerobic-heterotrophic growth yield ranges from 2.7 to 3.6 g cell/ave (Sasaki, Nishizawa, & Nagai, 1980); 'ave' stands for available electron from substrate, *e.g.* 8 mol e^- are available from 1 mol acetate.

1.1.2. Role of Photo-Pigments in Phototrophic Growth

Like plants, phototrophic bacteria harbor photosynthetic units that transform light energy is transformed into chemical energy. Instead of plant chlorophyll, phototrophic bacteria possess bacteriochlorophylls, which are located on their cell membrane. The photosynthetic units of each genus consist of different types of bacteriochlorophylls and carotenoids, and thus, have different absorption spectrum. Both carotenoids and bacteriochlorophylls are light harvesting pigments which are essential for light to chemical energy conversion, but their major role is different. Carotenoids are not only important in the light harvesting process (Codgell et al., 2006), but they are also essential in protecting the photosynthetic unit (Cogdell et al., 2000).

In the reaction center, the harvested light energy is transformed to chemical energy by photophosphorylation. Absorbed photons excite the bacteriochlorophyll molecules in the reaction center. The generated electron follows the cyclic electron flow to re-allocate protons from the cytosol to the periplasmic side of cell membrane. The proton gradient generated by this process drives the ATP synthesis. For more information of the light to energy conversion, see (Lodish et al., 2016).

1.1.3. Attenuation of Light

When light travels through any medium, whether fluid or solid, it interacts with the substances inside the media in many different ways depending on the chemical or physical properties of each substance. There are many modes of interaction between the particles and the travelling light. However, the only important light-particle interaction for light harvesting is absorption. Only this needs to be considered for their growth, since only the photons that have been absorbed can excite the bacteriochlorphyll and generate the electron flow. Only the light energy absorbed by the light harvesting complex can be utilized. Other interactions like scattering, reflection, diffraction, and others are not of interest since they do not contribute on the light to ATP conversion process. Nonetheless, these interactions with light have to be taken into account for an overview of light absorbance and dissipation effects, and to anticipate the efficiency of transfer of light quanta in a photobioreactor.

For the attenuation of light by biomass, it is possible to apply the Beer-Lambert law which is given as follows:

$$I = I_0 \cdot 10^{-A}$$

where A is absorbance [-], I_0 [W m^{-2}] is the incoming radiation, and I [W m^{-2}] is the transmitted radiation. The absorbance is not a single value but is proportional to a) the path length of light through the material, b) the concentration of absorbing substances in the material, and c) the molar, or mass, depending on the unit of concentration, attenuation coefficient of the attenuating substances in the material. The relationship is given as follows:

$$A = \varepsilon \cdot C \cdot L$$

where ε [m^2 g^{-1}] is mass attenuation coefficient, C [g m^{-3}] is mass concentration, and L [m] is path length. In case of multiple attenuating substances in a material, the total absorbance is the sum of absorbance of each substance. However, because mass attenuation coefficient changes with wavelength, the absorbance for each wavelength of light needs to be calculated. The above equation for single absorbing substance can be written considering the wavelength term as follows:

$$A(\lambda) = \varepsilon(\lambda) \cdot C \cdot L$$

To obtain the bulk absorbance, the above equation has to be summed with respect to all the wavelength of light provided and is given as follows:

$$A_{bulk} = \sum_{i=1}^{N} \varepsilon(\lambda_i) \cdot C \cdot L$$

1.2. Knowledge Gap

It is well known that PNSB need light as energy source and organic substrates as carbon source in photoheterotrophic growth. Numerous researches have been done with pure culture of either *Rhodobacter* or *Rhodopseudomonas* in their fundamental physiology.

However, the interaction of these organisms in a mixed-culture system of PNSB is not fully understood. Questions like influence of different light conditions or substrate type on the growth in mixed culture of PNSB are yet to be answered.

Various attempts have been made to investigate different light effect on their growth at different scales and operational mode with pure culture of PNSB (Aiking & Sojka, 1979; Carlozzi, Pushparaj, Degl'Innocenti, & Capperucci, 2006; Cornet & Albiol, 2000). In pure culture growth with different light intensities, PNSB has shown strong dependence of light intensity on their growth rate, and growth rate eventually saturates. However, the light intensity effects on a mixed culture PNSB under sequencing batch reactor (SBR) operation has not been revealed yet.

Although the characteristics of light harvesting pigments (*e.g.* bacteriochlorophylls or carotenoids) of PNSB have been extensively studied, the quantification of them has not been achieved in mixed culture and in relation to light intensity.

1.3. Research Questions and Hypotheses

Although many questions can arise from such knowledge gaps, the following three research questions have been selected and discussed in this work:

1. **What is the relationship between illumination characteristics and PNSB growth?**
2. **How would different illumination alter the content in light harvesting pigments and affect the growth rate of PNSB?**
3. **How and where can the relationship, light condition versus growth characteristics, be further utilized?**

The answer for the first question with natural sunlight has been already revealed (Carlozzi et al., 2006). However, in the current work artificial light was used to answer the question in a different way. Natural sunlight is relatively unstable and is a function of unpredictable weather conditions. In order to generate a stable illumination condition, artificial light has been used in a well-defined laboratory setting.

Light harvesting pigment content changes with available light intensity for pure culture of PNSB (Cohen-Bazire, Sistrom, & Stanier, 1957), however, a quantitative study of pigment content for mixed culture of PNSB and whether the production of photopigments is affecting the growth rate are still to be answered.

Accordingly, the following working hypotheses were postulated:

1. The growth rate will increase as more light is provided but will eventually face a saturation state where light intensity is not the limiting factor for growth
2. The bacteriochlorphyll content will increase inversely to light intensity change and growth rate will decrease as more substrates are allocated for pigments production and less light energy is provided.

As justification, an increase in light intensity translates into an increased photon flux, *i.e.* more photons and energy are emitted and transferred per time and area units ($W\ m^{-2} = J\ s^{-1}\ m^{-2}$), and thus to higher ATP generation per time unit. As more ATP is generated, more biomass will be generated per unit time which means the growth rate will increase. However, this growth rate will not increase forever as other nutrients necessary for building up cell materials will become limiting for the growth process.

The bacteriochlorophyll content of pure culture PNSB is inversely proportional to light intensity (Cohen-Bazire, Sistrom, & Stanier, 1957). This relationship would still hold in a mixed culture of PNSB, since the fundamental mechanism for pigment production remains identical.

2. Materials and Methods

The research questions were investigated by integrating wet-lab and dry-lab objectives with laboratory experiments and mathematical modelling, respectively: (A) growth of PNSB was studied in a mixed-culture SBR with four different light conditions; (B) a mathematical model was developed to simulate the growth of a model population of PNSB (*Rhodopseudomonas palustris*) in a pure culture subjected to the same light conditions used at wet lab. The main objective of simulation with pure culture *R. palustris* was to understand the fundamental behavior of these microorganisms and to compare with the outcomes of the mixed-culture experiment. Pure culture of *R. palustris* was chosen for the availability of growth kinetics data from earlier literature reports. The comparison between the two wet-lab and dry-lab works was expected to provide strong insights for a better understanding of the physiology of PNSB and their metabolic performance in a mixed-culture SBR under light intensity effects.

2.1. Growth of PNSB in a Mixed Culture under Different Light Conditions

Mixed culture. The mixed culture of PNSB was obtained from and maintained in a photo-bioreactor under operational conditions developed in the previous work of Stevens (Stevens, 2017) within the Weissbrodt Group. Prior to changing the light conditions, microbial community composition was analyzed. Biomass samples of 2 mL were centrifuged at 12,000xg for 5 min and the resulting supernatant was discarded. Genomic DNA (gDNA) was extracted from the centrifuged biomass using DNeasy® UltraClean® Microbial Kit (Qiagen, Germany) by following the manufacturer's manual. Concentration of extracted gDNA was quantified spectrophotometrically with Qubit 3.0 Fluorometer (Invitrogen, USA) following manufacturer's manual. Extracted gDNA samples were sent to Novogene (China) for 16s rRNA gene amplicon sequencing to identify the microbial composition of mixed culture PNSB.

Cultivation medium and growth condition. The mixed culture of PNSB was grown in a single-wall stirred-tank bioreactor (Applikon, Netherlands) with a vessel volume of 2.5 L and

working volume of 2.1 L. Cells were grown in a cultivation medium developed by Stevens (2018) and the final composition is given in table 1.

Table 1. Growth medium, vitamin solution and trace element solution composition. Since both the medium is not sterilized, carbon source is separated from the nitrogen and phosphorous source to prevent microbial growth in medium. This medium was provided to the reactor.

Final Composition of Growth Medium

	Chemical Formula	Concentration	Note
C – source Stock solution	$CH_3COONa \cdot 3H_2O$	0.914 g L^{-1}	0.397 g L^{-1} as Acetate (430 mg COD L^{-1})
	$MgSO_4 \cdot 7H_2O$	0.200 g L^{-1}	
	$CaCl_2 \cdot 2H_2O$	0.05 g L^{-1}	
	NaCl	0.2 g L^{-1}	
N & P – source Stock solution	KH_2PO_4	0.014 g L^{-1}	0.021 g L^{-1} as Phosphate (6.85mg P L^{-1})
	K_2HPO_4	0.021 g L^{-1}	
	NH_4Cl	0.229 g L^{-1}	0.077 g L^{-1} as Ammonium (59.76 mg N L^{-1})
	Vitamin Solution	1 mL L^{-1}	
	Trace Element Solution	1 mL L^{-1}	
Composition of Vitamin and Trace Element Solutions			
	Elements	Concentration	Note
Vitamin Solution	Thiamine-HCl	200 mg L^{-1}	Vitamin B_1
	Niacin	500 mg L^{-1}	Vitamin B_3
	p-amino benzoic acid	300 mg L^{-1}	Bacterial Vitamin
	Pyridoxine-HCl	100 mg L^{-1}	Vitamin B_6
	Biotin	50 mg L^{-1}	Vitamin B_7
	Vitamin B_{12}	50 mg L^{-1}	
Trace Element Solution	$EDTA\text{-}2Na \cdot 2H_2O$	110 mg L^{-1}	
	$FeCl_3 \cdot 6H_2O$	2000 mg L^{-1}	
	$ZnCl_2$	100 mg L^{-1}	
	$MnSO_4 \cdot H_2O$	64 mg L^{-1}	
	H_3BO_3	100 mg L^{-1}	
	$CoCl_2 \cdot 6H_2O$	100 mg L^{-1}	
	$Na_2MoO_4 \cdot 2H_2O$	24 mg L^{-1}	
	$CuSO_4 \cdot 5H_2O$	16 mg L^{-1}	
	$NiCl_2 \cdot 6H_2O$	10 mg L^{-1}	
	$NaSeO_3$	5 mg L^{-1}	

Since the medium was not sterilized, to minimize microbial growth in media, carbon source was separated from nitrogen and phosphorous source. Vessel was sparged with pure

argon gas to maintain anaerobic conditions and was illuminated with two halogen lamp floodlights (Gamma, Netherlands) of 120W each from opposite directions. Light intensity was tuned by a light dimmer and the power consumption was monitored by an energy monitor (EM-16, Alecto, Netherlands). Emitted light was filtered with an interference filter (Black Perspex 962, Plasticstockist, UK) allowing only near IR spectrum to pass (>700 nm). Culture was maintained at 30°C and pH 7.

Adjustment of pH was done with either 1 mol L^{-1} of HCl or 1 mol L^{-1} of NaOH stock solutions. Sludge retention time was managed to 40 h and biomass concentration was maintained below 1.2 g VSS L^{-1}. As the results from Katsuda et al. (2002) shows, the correlation of light attenuation model they have used has good agreement with their experimental results at a biomass concentration below 1.2 kg dry cells m^{-3}. Thus, in the present study, the biomass concentration was also maintained below 1.2 g VSS L^{-1} to roughly keep the good agreement Katsuda et al. (2002) obtained as the model used in the present study was a modification of their work.

Reactor infrastructure. The photo-bioreactor consisted of a cylindrically shaped vessel with a curved bottom made of borosilicate glass (transmittance≥90% in the wavelength range of the filtered light). Reactor was equipped with a pH probe, temperature probe, redox probe, dissolved oxygen probe, and was stirred with an anchor stirrer. Silicon blades were attached to the anchor stirrer to wipe the inner surface of the reactor and minimize biofilm growth on the reactor surface which can severely interfere the penetration of light into the reactor. Residual biofilm growth on probes and stirrer was removed once in every week by opening the reactor; cleaning time was suppressed to maximum 10 minutes. The reactor was operated in SBR mode with an 8 h cycle composed of 3 h of settling, 5 min of discharge of 640 mL of supernatant after settling, 5 min of idle, 5 min of charging 1050 mL of medium, 281 min of reaction, and 4 minutes of purging 310 mL of mixed culture. Five samples of each 20 mL were taken in every reaction phase with 70 min interval. During stabilization period of one week after altering the light intensity, no samples were taken and the discharge volume was increased to 740 mL instead of 640 mL.

Floodlights were placed 20 cm away from the reactor surface on opposite side and the measured light intensity at the surface of the reactor was 350 W m^{-2}. The entire setup was placed inside a hood with windows covered with black low-density polyethylene films to block external light. External light was blocked in order to have a controlled illumination condition and, additionally, prevent other phototrophs from growing. Temperature of the culture was

maintained at 30°C with a thermostat (WK 500, Lauda, Germany) providing coolant to a finger type heat exchanger (Applikon, Netherlands). Exhaust gas from the reactor went through a condenser (Applikon, Netherlands) provided with coolant of 5°C using a thermostat (RMS6, Lauda, Germany) in order to obtain dry exhaust gas.

Light measurement. Incident light intensity was measured with a pyranometer (CMP3; Kipp & Zonen, The Netherlands) at the surface of the reactor. Light intensity was changed by a light dimmer and the energy consumption was monitored in correlation to the light intensity. Light intensity of 350 W m^{-2} was set as a baseline to monitor the effect of light intensity on the growth and nutrient removal of mixed culture PNSB. Such intensity was obtained on two opposite side of the reactor with each flood lamps being 20 cm away from the reactor with the filter located in between the reactor and the lamps. The baseline light intensity is the maximum output of each flood lamps and could only be decreased from that value. To control the light intensity, the connected dimer was tuned and the connected energy monitor was used to convert the energy consumption readings to light intensity with the obtained calibration curve. The calibration of energy consumption to light intensity can be found in the appendix. The four settings correspond to 350 W m^{-2} (100%), 262.5 W m^{-2} (75%), 175 W m^{-2} (50%), and 87.5 W m^{-2} (25%); percentage inside the brackets indicate the ratio of each setting to 350 W m^{-2} as base. These four settings were empirically chosen.

Growth measurement. Growth of cells was determined by spectrophotometry (Libra S11; Biochrom, UK). Biomass dry weight was simultaneously measured to translate absorbance to g VSS L^{-1} using a calibration line. Samples of known volume were first centrifuged at 12,000xg for 5 min and after removing the supernatant, were dried on glass fiber filter membrane at 105°C for 24 h. Dried samples were burned in the oven at 550°C for 2 h. Residual ash weight was measured and the VSS was calculated as follows:

$$\boldsymbol{VSS} = \frac{[(\boldsymbol{Dry}-\boldsymbol{Empty})-(\boldsymbol{Ash}-\boldsymbol{Empty})]}{\boldsymbol{Sample\ Volume}} \quad (1)$$

where' 'Dry' is weight of dried sample, 'Empty' is weight of empty filter membrane and 'Ash' is residual ash weight.

Settling rate was measured as follows:

$$Settling\ Rate = (X_{p,end} - X_{p,eff})/t_{set} \quad (2)$$

where $X_{p,end}$ is the biomass concentration at the end of reaction phase, $X_{p,eff}$ is the biomass concentration of the effluent, and t_{set} is the settling time of 3 h.

Nutrient removal and photo-pigments. Ammonium and phosphate were measure with a discrete analyzer (Gallery™ Automated Photometric Analyzer; Thermo Scientific, USA), and acetate was measure with a high-performance liquid chromatography (HPLC) system. The HPLC system consisted of an autosampler (2707 Autosampler, Waters, USA), a refractive index detector (2414 Refractive Index Detector, Water, USA), and an absorbance detector (484 Tunable Absorbance Detector, Waters, USA). Column used in the system was HPX-87H (300x7.8 mm, Cat no. 1250140; Bio-Rad, USA) with a pre-column of Cation-H refill cartridge (30x4.6mm, Cat no. 1250129, Bio-Rad, USA), H_3PO_4 (1.5 mmol L^{-1}) was used as eluent with a flow rate of 0.6 mL min^{-1} and column temperature was maintained at 59°C. Injection volume of each sample was set to 10 µL at 15°C. All 5 points in reaction phase were analyzed to track the nutrient removal rate.

Quantification of light harvesting pigments was done by both reverse phase HPLC (RP-HPLC) and microwell plate reader, after extraction from the cell membrane of the PNSB-based biomass. Biomass samples of 2 mL were first centrifuged at 12,000xg for 5 minutes. Supernatant was discarded and remaining pellets were re-suspended in 2 mL of extraction solution composed of acetone and methanol (7:2 v/v), and were sonicated to increase extraction efficiency. Sonication was done with a sonicator (Sonifier S-250A, Branson Ultrasonics) for 30 seconds with the following settings: output control level 3, duty cycle 20, 30, and 40%. Output control level 3 corresponded to 20W, and duty cycle is the ratio of sonication time to total operation time; duty cycle of 20% means of total operation time, 20% of time sonication was applied. Extraction was performed in cold-dark room (<5°C, very dim light) to minimize photo-oxidation of bacteriochlorophyll to bacteriopheophytin. Only during the sonication process, samples were exposed to light for a practical limitation: sonicator could not be located in the cold-dark room. After sonication, the solution was set to rest for 60 minutes and then centrifuged at 12,000xg for 5 minutes again to settle down remaining cell debris. The supernatant was collected and filtered with a 0.2 µm syringe filter. For spectrophotometric quantification, 200µL of samples were transferred to polypropylene micro well plates (96 well, PP, F-Bottom; Greiner Bio-One, Austria) and examined with a well plate reader (Synergy™ HTX Multi-Mode Reader; BioTek, USA). To prevent evaporation of extract solvent during micro plate reading, micro well plates were covered with optically transparent seal films (Optical tape #223944, Bio-Rad, USA). Transparent polypropylene micro well plates were used instead of polystyrene plates because the extraction solvent consisted of acetone which damages polystyrene. The concentration of bacteriochlorophyll was calculated by measuring

absorbance and path length with reported molar absorption coefficients in acetone/methanol solution: BChl a, 65.3 [L $mmol^{-1}$ cm^{-1}] (van der Rest & Gingras, 1974).

In addition to the spectrophotometry for pigment quantification, RP-HPLC system was also used. The RP-HPLC system consisted of a reversed-phase C_{18} column (Nova-Pak C18; 60Å, 4 µm, 3.9 mm x 300 mm, Waters, USA) with a pre-column, a photodiode array detector (996 Photodiode Array Detector; Waters, USA), and the flow was regulated by a separation module (2695 Separation Module, Waters, USA). The method used was followed as previously described (Frigaard, Takaichi, Hirota, Shimada, & Matsuura, 1997). Presence of bacteriochlorophyll was identified by comparing the retention times with the bacteriochlorophyll standard purchased from Sigma-Aldrich and the concentration was calculated by comparing the HPLC peak area with that of the standard. The signal from photodiode array detector was integrated and the peak area was converted to concentration by the calibration result of standard. Signal was monitored at two different wavelengths, 270nm and 363nm, and calibration was made for both wavelengths; 270 nm as used in the method described by Frigaard et al. (1997) and 363 nm as it is a characteristic peak of bacteriochlorophyll a in extraction solvent used. Manual integration was required in some cases and the integration for these was based on matching the retention time with the standard. For each setting, samples were processed in two groups: first group consisted of start and end of each cycle, and the second group was the rest. This separation was done intentionally to process the samples by plate reader and RP-HPLC system simultaneously and minimize time lag between the two different analyses that might cause bias by oxidation of extracted pigments. Due to limitation of throughput in the RP-HPLC system used, mainly the operation time and eluent consumption, only two samples, start and end, of each cycle at different light settings were examined.

2.2. Light Distribution in the Photobioreactor and Growth Simulation

Growth simulation with Aquasim was performed to understand the deviation from modelling to experimental data and to obtain parameters like half velocity coefficients (K_{ac}, K_{am}, K_I). In order to simulate the complex growth characteristics of mixed culture PNSB, some assumptions had to be made. First, since a mixed culture consists of diverse populations and each has different growth kinetics, it was simplified to a simple model single culture system with known parameters. For this assumption, *Rhodopseudomonas palustris* was chosen, which has available data from a previous work (McKinlay & Harwood, 2010) on top of the genus

Rhodopseudomonas being a predominant member of the studied mixed culture as it will be shown later in figure 4. Secondly, simulation was simplified by only using acetate and ammonium as substrate for growth. Thirdly, provided light energy was assumed to be uniform in vertical direction, and attenuation by the components of the reactor (*e.g.* glass wall, probes, stirrer, etc.) and medium were neglected.

2.2.1. Reactor Geometry

Cylindrical reactor was chosen for simulation to match with the wet lab settings. Light was assumed to be provided uniformly on the surface of the reactor, *i.e.* irradiance at any point of the reactor surface is identical. The geometry of the used reactor in simulation can be seen in figure 1.

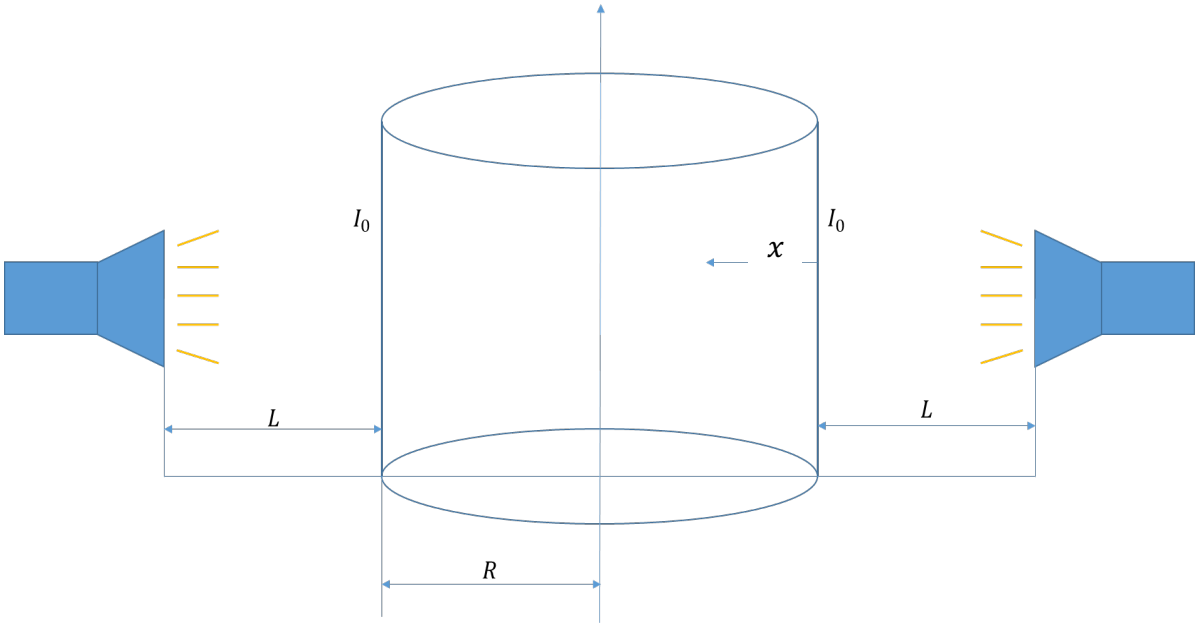

Figure 1. Geometry of photobioreactor used in this study. The reactor radius is 'R', intensity of light measured at the surface of reactor is '$\boldsymbol{I_0}$', distance from the reactor to the light source is 'L', and 'x' is the distance from the surface of the reactor to a point inside the reactor.

2.2.2. Attenuation model

Emitted light from both flood lights travels through air and transmitted through the glass wall of the reactor. By transmitting through the glass wall, light is attenuated and its intensity decreases depending on the attenuation properties of the materials the glass wall is composed of. As mentioned, every material has its own absorption spectrum. For this, it is important to express light intensity equations in a wavelength term. The attenuation model here described

is an adaptation of the works of Katsuda et al. (Katsuda, Fujii, Takata, Ooshima, & Katoh, 2002).

Let us denote the spectral irradiance of wavelength λ measured at the outer surface of the reactor wall as $I_{0,\lambda}$ and the intensity measured at the inner surface of the reactor as $I'_{0,\lambda}$. Each term $I_{0,\lambda}$ and $I'_{0,\lambda}$ are spectral irradiances at wavelength λ which is in the spectrum range of emitted light from flood lights. In the simulation the attenuation by glass wall was neglected for the unavailability of instruments for measuring the attenuation profile of the glass wall. Albeit its importance, this assumption is reasonable in a sense that the reactor wall used in this study was made of borosilicate glass, which has very high transmittance (~90%) in the spectrum range of our operation of filtered light (> 700nm). The spectral irradiance data of the filtered light can be seen in the appendix.

Since light is coming from both direction and each travel different path length to reach the same position, the intensity obtained at that position is the sum of each intensity from both directions.

$$\boldsymbol{I_{blank,\lambda} = I_{blank,right,\lambda} + I_{blank,left,\lambda}} \tag{3}$$

Here each subscript 'right' and 'left' refers to the two directions of incoming light, respectively and blank refers that there is no culture present in the reactor. When light travels through a distance, its intensity naturally decreases due to dispersion, so the light intensity measured at the surface of reactor, $I_{0,\lambda}$, is higher than the intensity, $I_{blank,\lambda}$, measured at a distance 'x' away from the surface. Applying an energy balance at the surface of reactor and an imaginary plane in the reactor at distance 'x', the following two equations can be obtained:

$$\boldsymbol{4\pi L^2 I_0 = 4\pi (L_0 + x)^2 I_{blank,right,\lambda}} \tag{4}$$

$$\boldsymbol{4\pi L^2 I_0 = 4\pi (L_0 + 2R - x)^2 I_{blank,left,\lambda}} \tag{5}$$

where x is the distance from the light source to the reactor surface and R is the radius of the reactor. The above equation comes from the inverse square law stating that radiation intensity has an inverse proportionality to the square of the distance from the source. In the presence of culture which attenuates light, intensity of each light is assumed to follow the Beer-Lambert's law; this can be expressed as follows:

$$\boldsymbol{I_{right,\lambda} = I_{blank,right,\lambda} \cdot 10^{-\varepsilon_{cell,\lambda} \cdot C \cdot x}} \tag{6}$$

$$\boldsymbol{I_{left,\lambda} = I_{blank,left,\lambda} \cdot 10^{-\varepsilon_{cell,\lambda} \cdot C \cdot (2R - x)}} \tag{7}$$

where C is the biomass concentration in the culture and $\varepsilon_{cell,\lambda}$ is the spectral mass attenuation coefficient of cell. Attenuation coefficient is expressed in wavelength just like intensity is for

the same reason mentioned above for intensity. With the same principle we have used to formulate equation (1), the following can be obtained:

$$\boldsymbol{I_{\lambda} = I_{right,\lambda} + I_{left,\lambda}} \quad (8)$$

where I_{λ} is the intensity obtained at distance 'x' from the reactor surface with the biomass concentration.

Now combining equations (2) to (6), the spectral irradiance at a point with distance 'x' away from the surface of the reactor with attenuation and dispersion of energy considered can be obtained.

$$\boldsymbol{I_{\lambda} = \left(\frac{L}{L+x}\right)^2 I_{0,\lambda} \cdot 10^{-\varepsilon_{cell,\lambda} \cdot C \cdot x} + \left(\frac{L}{L+2R-x}\right)^2 I_{0,\lambda} \cdot 10^{-\varepsilon_{cell,\lambda} \cdot C \cdot (2R-x)}} \quad (9)$$

Since the equation (7) is only calculating the intensity at wavelength λ, to get the total intensity, it needs to be integrated for all the wavelength of our interest.

$$I = \sum_{\lambda} I_{\lambda} = \sum_{\lambda} \left[\left(\frac{L}{L+x}\right)^2 I_{0,\lambda} \cdot 10^{-\varepsilon_{cell,\lambda} \cdot C \cdot x} + \left(\frac{L}{L+2R-x}\right)^2 I_{0,\lambda} \cdot 10^{-\varepsilon_{cell,\lambda} \cdot C \cdot (2R-x)} \right] \quad (10)$$

The above equation is only valid when every cell is immobilized to its original position. However, since the culture is continuously mixed in order to minimize unequal substrate distribution, approximation is needed to imitate the situation. Assuming that the mixing is perfect, *i.e.* perfect equality in substrate supply for each cell, it is possible to think that in a very short time interval each cell in the culture is experiencing every light intensity available inside the reactor. With this assumption, it is possible to say that the light intensity every cell is receiving is simply the average value of all the light intensities inside the reactor. As a result, the average intensity a cell receives can be expressed as follows:

$$I_{avg} = \frac{1}{R} \int_0^R I dx \quad (11)$$

Such approach of using average light intensity is more representing the actual light condition in the reactor (Camacho-Rubio et al., 1985, Ogbonna & Tanaka, 2000). Usage of incident light intensity is only valid in systems of very shallow light path and low concentration, so for the system used in the present study, the average light intensity approach is more realistic. A computational script for obtaining the average intensity in a reactor with given biomass concentration can be found in the supplementary materials.

2.2.3. Growth kinetics and Stoichiometry

Kinetics and Conversion

Biomass specific growth rate and biomass specific nutrient removal rates were calculated to compare the effect of altering light intensity on their performances. For better comparison, instantaneous biomass specific growth rate was calculated at the beginning of reaction phase rather than the average biomass specific growth rate for the whole reaction phase. Instantaneous biomass specific growth rate (μ_{ini}) was calculated with the following formula:

$$\mu_{ini} = \frac{dX_p}{dt}_{t=0} / X_{p,start} \quad (12)$$

where $X_{p,start}$ is the biomass concentration at the start of reaction phase.

Instantaneous biomass specific nutrient removal rate at the beginning of reaction phase was calculated as follows:

$$r_{S_i} = \frac{dS_i}{dt}_{t=0} / X_{p,start} \quad (13)$$

where S_i can be any substrate.

For obtaining the instantaneous biomass growth rate and nutrient removal rate, experimentally obtained biomass and substrate concentration data were fitted using the Curve Fitting Toolbox in Matlab. For all cases, fitted equations had the exponential form of $a \times \exp(b \times t) + c \times \exp(d \times t)$, where a, b, c, d are constants and t is reaction time. From the obtained formulas by curve fitting, the instantaneous rates were calculated at the starting point of each reaction cycle.

Biomass yield on acetate, ammonium, and phosphate were calculated at the initial point of reaction by comparing the biomass rate to substrate consumption rate and they were calculated with the following formula:

$$Y_{X_p/S_i} = \mu_{ini}/r_{S_i} \quad (14)$$

2.2.4. Model implementation in Aquasim assisted by Matlab

Aquasim is an open software for computer modelling of aquatic system developed by Reichert (Reichert, 1994). Simulation is imitating the conditions applied in wet lab experiments. The same operational setting was used in the simulation. Average light intensity relationship with biomass concentration was first calculated with the Matlab script mentioned above and then implemented in Aquasim. Acetate and ammonium dosing concentration, 396.6

mg L^{-1} and 77.2 mg L^{-1}, respectively, was originally calculated from the wet lab medium composition. Other parameters, such as K_{ac} (0.5 mg Ac L^{-1}), K_{am} (2 mg Am L^{-1}), or K_I (20W m^{-2}), were chosen arbitrary based on the wet lab results. Maximum specific growth rate (μ_{max}) was set to 0.0825 h^{-1}, and biomass yield on acetate (0.665 g VSS g Ac^{-1}) and ammonium (6.91 g VSS g Am^{-1}) were calculated from the chemical composition of *Rhodopseudomonas palustris* which were obtained from published work (McKinlay & Harwood, 2010).

Biomass growth kinetic was assumed to follow Monod type with acetate as carbon source, ammonium as nitrogen source, and average light intensity as additional substrate term. The assumption of using light intensity as a substrate term has already been used (Cornet & Albiol, 2000; Puyol, Barry, Hülsen, & Batstone, 2017). One thing to notice here is that albeit light intensity is used as a substrate term, it should not be considered as a real substrate. Unlike carbon source or nitrogen source, light intensity does not contribute on the stoichiometry of growth, but only on the rate of growth since they are not building materials of a cell. The biomass specific growth rate (μ) is formulated as follows:

$$\mu = \mu_{max} \cdot \frac{S_{ac}}{K_{ac}+S_{ac}} \cdot \frac{S_{am}}{K_{am}+S_{am}} \cdot \frac{S_I}{K_I+S_I} \quad (15)$$

where μ_{max} is maximum biomass specific growth rate. Full script of the model can be found in the appendix.

3. Results and Discussion

3.1. Light Distribution and Growth Simulation

Light distribution inside a photoreactor

Prior to simulation of light attenuation, absorbance spectrum of the biomass was measured to calculate the mass extinction coefficients of the bulk biomass. In order to obtain the average light intensity profile in the reactor with given incident light intensity, the first step was to obtain the mass extinction coefficient of cell at each wavelength. With known biomass concentration, *in vivo* mass extinction coefficient in water was obtained as shown in figure 2. The mass extinction coefficient was only calculated in the region from 300 nm to 1000 nm. The UV region was not calculated as the micro well plate used were made of polystyrene which shows high absorbance in that region. The relatively higher absorbance above 900 nm comes

from the absorption by water. From the obtained spectral mass extinction coefficient ($\varepsilon_{cell,\lambda}$) the average light intensity was calculated by eq. (8) and eq. (9) with given reactor geometry.

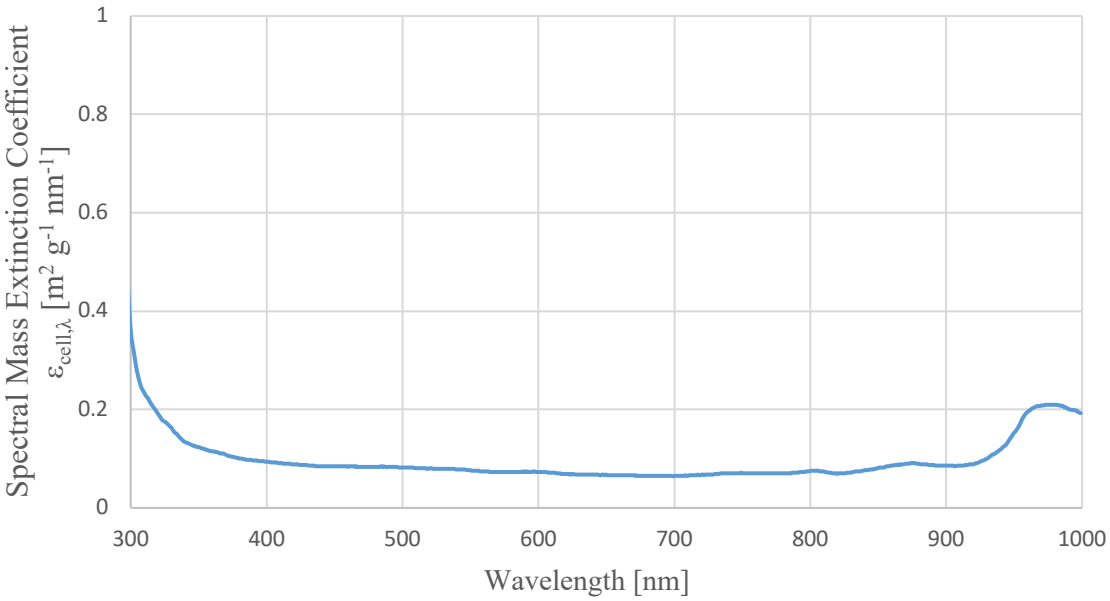

Figure 2. Mass extinction coefficient of the PNSB mixed culture at different wavelength.

Simulation of light attenuation done with Matlab to obtain the light distribution profile in a photo-bioreactor is shown in Figure 3. Figure 3 shows the result of light distribution inside the reactor at different biomass concentration with the incident light intensity of 350 W m^{-2}. As it can be seen from the figure, light intensity decreases away from the reactor surface. At higher biomass concentration it can be noticed that the intensity decreases more rapidly with increasing distance from the reactor surface.

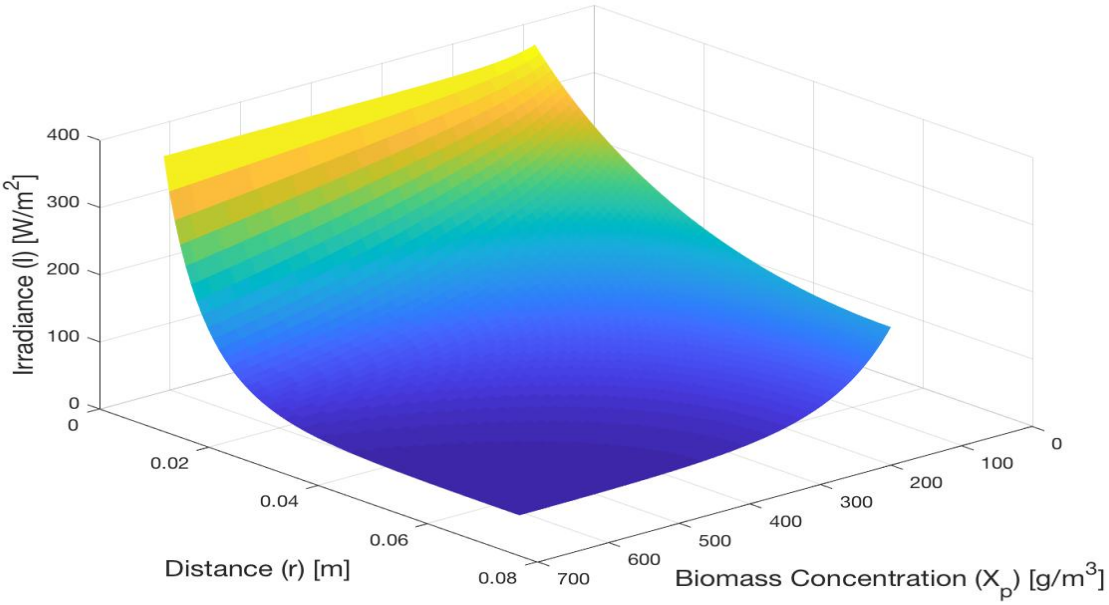

Figure 3. Calculation result of irradiance at a given distance with given biomass concentration. Distance (r) is the distance from the surface of the reactor wall to a given point and the biomass concentration is the bulk concentration of the culture.

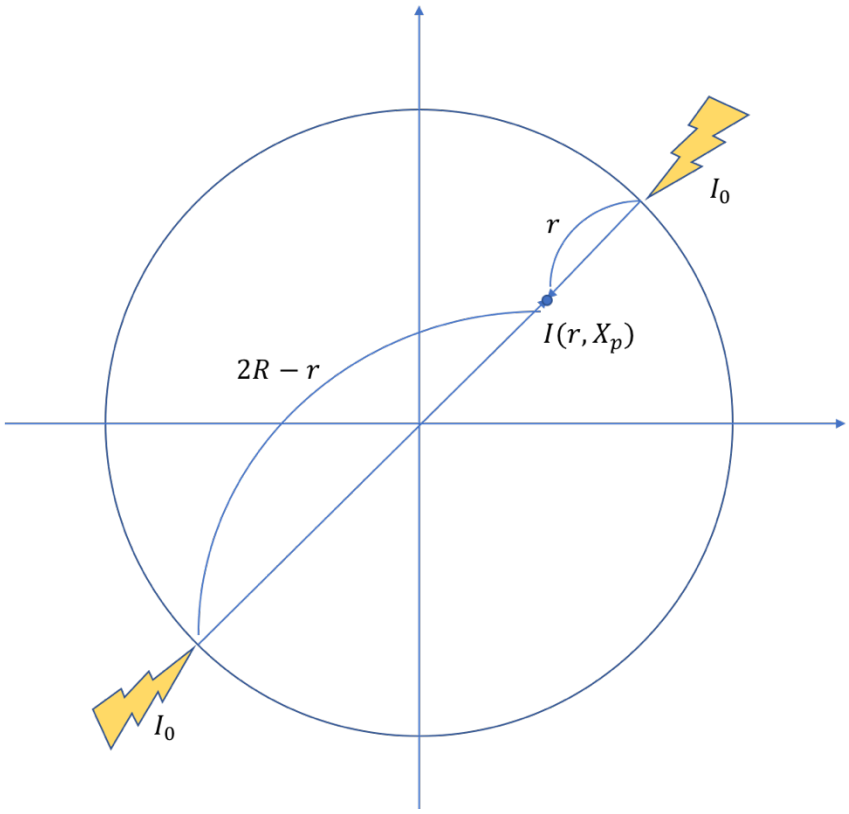

Figure 4. Reactor geometry from top view. $\boldsymbol{I_0}$ [W m^{-2}] is incident light intensity, $\boldsymbol{r}$ [m] is distance from the reactor surface to a point, $\boldsymbol{I(r, X_p)}$ is the light intensity obtained at that point with given biomass concentration $\boldsymbol{X_p}$ [g VSS L^{-1}], and $\boldsymbol{R}$ [m] is radius of the reactor.

Figure 3 gives useful information for the operation of an immobilized system where microorganisms are fixed to their position, or the system is static. In such systems, the penetration of light is limited to the area close to the surface and only in that region phototrophs can obtain enough light energy for growth. The width of the region will strongly be dependent on the biomass concentration and the incident light intensity. The unbalanced distribution of light will result such that phototrophic organisms will be located close to the surface of the reactor where they have sufficient light energy and non-phototrophic organisms will be located towards the center of the reactor. To prevent such segregation and obtain a homogenous culture, the system is continuously mixed to distribute light as uniform as possible. By mixing the culture, the dependence of position in the light distribution model is eliminated as cells experience every light intensity in the reactor and the average light intensity becomes more useful than the incident light intensity.

From the distribution of light in figure 3, the average light intensity equations by curve fitting were firstly obtained. The fitted equations were then implemented in the Aquasim

simulation and the simulation results are shown in the following section with the wet lab results for comparison.

3.2. Mixed Culture PNSB Wet-lab Experiment

Prior to proceeding experiments, it was necessary to identify the microbial community composition of the mixed culture and verify the dominance of PNSB. The following figure 5 shows the microbial community of the mixed culture after the stabilization period 1 month prior to baseline measurement. Operational condition was maintained stable until the start of baseline measurement. Microbial community composition of four different light intensity conditions are to be delivered in the coming future and thus, are not present in this report.

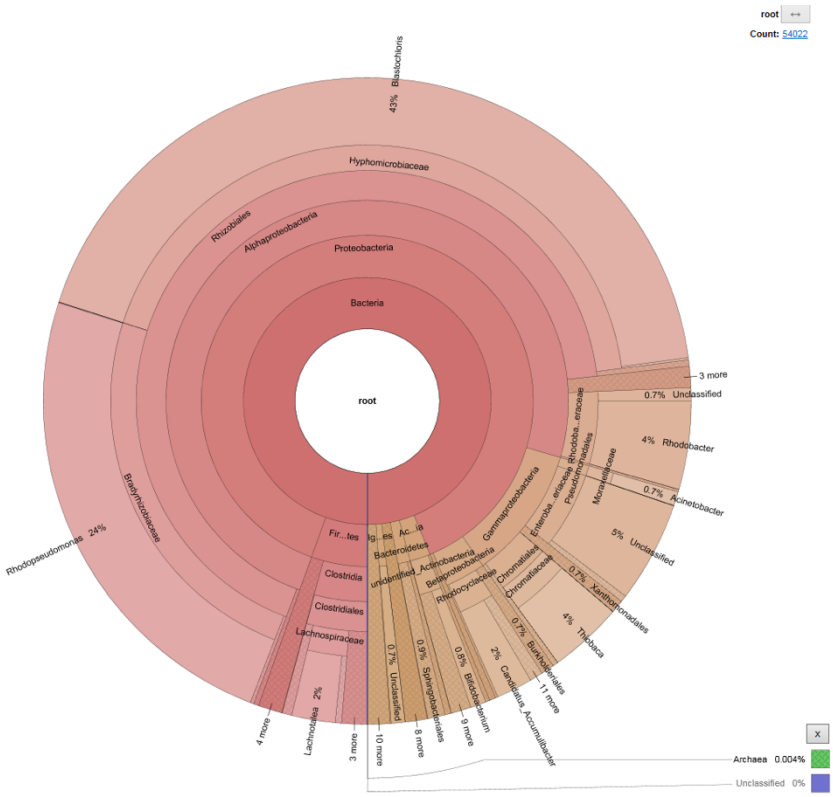

Figure 5. Microbial community composition of mixed culture PNSB before the start of light intensity adjustments. Composition is given in relative dominance. Representative genera of PNSB are *Blastochloris*, *Rhodopseudomonas*, and *Rhodobacter*.

From figure 5 it can be seen that the community is dominated by PNSB, taking up to 71% of total population in the mixed culture. The operational condition at the point of sample consisted of the above community was maintained until the beginning of baseline condition. It is of uncertainty whether the community composition has significantly changed or not before

the baseline condition sampling, however, it is most likely in the absence of any condition change acting as a driving force for community change, the composition remained steady.

3.2.1. Light Intensity Effect on Growth and Nutrient Removal

The photo-bioreactor was continuously operated with the 8 h cycle at 4 different light intensities from 350 (100%) to 262.5 (75%), 175 (50%), and 87.5 (25%) W/m^2 to check their effect on the growth and nutrient removal. For each intensity setting, 4 cycles were analyzed to minimize sampling error and 5 samples with constant time interval in each cycle were taken to obtain enough data to track the growth and nutrient removal. Due to time limitation, microbial community change in the four light conditions were not examined.

Rapid growth and nutrient removal at baseline condition (100% intensity, 350 W/m^2)

Biomass concentration was measured by absorbance at 660 nm and converted to VSS [g L^{-1}] by the calibration curve in appendix. Absorbance measured at 660nm was translated to cell density (Meyer, Kelley, & Vignais, 1978; Schultz & Weaver, 1982; Uyar, Eroglu, Yücel, Gündüz, & Türker, 2007). Biomass growth curve in figure 6 shows rapid increase in the first 140 minutes and then reaches a plateau with a final concentration of 0.52 g VSS L^{-1}. The plateau indicates that the biomass did not grow further than that level, which means the growth is limited. Before going into discussing limiting substrate for growth, it is of importance to clarify the term limiting substrate. The term 'limiting substrate' can be defined for both growth rate limiting and growth yield limiting in a batch culture. From here on both growth rate-limiting and growth yield-limiting will be used and as their name indicates, they have different meanings.

The figure 7 shows each substrate concentration trend in the reaction phase of 281 minutes for four different light intensity conditions. As it can be seen from figure 7 **a**, acetate concentration in baseline condition shows rapid consumption for the first 70 minutes and the consumption stopped at 19.9 mg Ac L^{-1}, whereas it can be seen in figure 7 **b** and 7 **c** for ammonium and phosphate, respectively, both are not fully consumed. One thing to notice is that even though acetate concentration is not changing, *i.e.* it is not consumed anymore, ammonium concentration and phosphate concentration keeps decreasing, which means they are consumed. One possible reason for this is the use of Calvin cycle for recycling the reduced redox cofactors generated during acetate oxidation and maintain redox balance in the cell (McKinlay & Harwood, 2010). As Calvin cycle runs to maintain redox balance, carbon dioxide

generated in the oxidation process of acetate is fixed into cell material, and the consumption of ammonium and phosphate for biosynthesis of cell materials can be explained. This also explains the slight increase of biomass concentration after the stop of acetate consumption. However, further investigation is necessary to validate this.

From table 2 it can be seen that the initial concentration measured in the samples were lower than the theoretical concentration of the substrates in the medium. This can be due to 1) nutrient dosing pump was off set, and 2) dilution by remaining bulk liquid. The targeted volume after removal of supernatant is 1.05 L and the inflow volume was set to 1.05 L so that the working volume meets 2.1 L. Expected acetate concentration after inflow, if acetate is fully consumed before the dosing, is 198.29 mg L^{-1} whereas the actual value was 95.5 mg L^{-1}. This shows that the nutrient pump was not properly set and only about 44% of the targeted inflow rate was operated. Ammonium and phosphate were also not fully provided.

In table 2, the initial and final concentration of biomass, and three substrates are shown. A simple mass balance for the substrates mentioned in table 2 shows an unrealistic result. The biomass change is about 126.4 mg L^{-1} and the change of three main substrates (acetate, ammonium, and phosphate) is in total about 85.67 mg L^{-1} (75.6 mg Ac L^{-1} + 9.02 mg NH_4^+ L^{-1} + 1.05 mg PO_4^{3-} L^{-1}); concentration comparison is valid since the working volume does not change in the reaction phase. It is most likely that the substrate measurements show smaller error than that of the biomass concentration which is obtained from the conversion of absorbance to VSS. The absorbance to biomass concentration conversion figure in appendix shows a low R^2 value indicating the correlation is poor. Such poor R^2 value increases the error incorporated in the conversion of measured absorbance to VSS. Overestimation of biomass concentration is most likely the reason for such imbalance in mass.

Slight decrease of growth and nutrient removal rate at 75% Intensity (262.5 W m^{-2})

From the baseline setting, only incident light intensity was changed from 350 W m^{-2} to 262.5 W m^{-2}. Just like the baseline condition where biomass growth was saturated before the end of reaction phase, in the 75% condition, the same saturation trend can be seen in figure 6 at around 140 min. This indicates, as mentioned before in the baseline setting section, growth is limited by one substrate or more. The starting biomass concentration was about 9% lower than that of the baseline condition. This was mainly, as it will be discussed later, due to the change of biomass settling rate.

Ammonium consumption is an indication for biomass growth in this culture since it was the only nitrogen source in the system and conversion ratio of ammonium to biomass

should be more or less the same as it is most likely that the presence of nitrifiers can be excluded, *i.e.* all ammonium should be incorporated in biomass conversion but not used as an energy source.

In figure 7, concentration change of all three substrates at 75% intensity condition can be seen. Acetate consumption shows slightly different trend to that of baseline condition as the residual concentration at time 70 minutes is higher than it is in the previous setting. The concentration reaches the plateau at around 140 minutes unlike it is 70 minutes in baseline result. The time delay in reaching the plateau means the acetate consumption rate is decreased. However, whether this decrease is solely due to the decrease of light intensity or due to higher biomass concentration will be discussed later in this section. The same unknown further consumption of ammonium and phosphate after full consumption of acetate is still present in the result.

Initial concentration of ammonium and phosphate have slightly increased than the baseline condition. This is mainly due to higher residual concentration of each substrate at the end of reaction phase which eventually accumulated in the system and increased the initial concentration even if the substrate dosing rate remained constant. In table 2 it can be seen that ammonium and phosphate removal ratio in 75% intensity condition have decreased compared to the baseline result. Acetate, however, shows almost the same removal ratio as baseline result.

In figure 8, the average light intensity change during the reaction phase of 75% light intensity condition is shown. The values were computed with eq.(11) and shows a saturation trend. This saturation of $I_{avg}$is obvious as the eq.(11) is a function of biomass concentration, which shows a saturation curve in figure 7.

Further decrease of growth & nutrient removal at 50% intensity (175 W m^{-2})

Light intensity was decreased to 50% of its original, 175 W m^{-2}, and was calculated from the calibration curve in appendix same as before. Sludge retention time was maintained to the same level (~40 hours) as the previous settings. In figure 6, again, biomass concentration reaches saturation, however, in this condition they reach such point slightly later than the previous two cases. This is confirmed by the substrate concentration change shown in figure 7. In this setting, it is more obvious that the other two substrates, ammonium and phosphate, are further consumed by the culture as it can be seen in figure 7. Acetate consumption stops at around 140 minutes, but ammonium and phosphate concentration keep decreasing even after

that point. The reason for such continuous consumption needs further investigation due to limited information.

Compared to the previous two settings, phosphate removal ratio has decreased from 52% to 27%, and ammonium removal ratio has also decreased from 32% to 23%, whereas the acetate removal ratio has barely changed. In higher incident light intensity, the mixed culture can remove ammonium and phosphate better than in lower intensity. This has mainly due to higher biomass concentration in the high intensity conditions resulting in better removal ratio. For acetate this can't be observed since it is already reaching saturation before the end of reaction phase.

Significant growth & nutrient removal decrease at 25% intensity (87.5 W m^{-2})

The final setting was set to 25% of incident light intensity which corresponds to 87.5 W m^{-2}. With this intensity, it can be seen from figure 6 that biomass growth is not reaching a saturation level as observed in previous settings. The biomass concentration steadily increases until the end of the reaction phase. The relatively larger error bars in the figure indicates that the biomass concentration shows large deviation among each cycle and this is mainly due to biomass loss in the effluent flow. As it will be explained in the end of this section, the change in settling rate has significant influence on the initial biomass concentration. For now, in short, the decrease in settling rate is the main reason for such decrease in initial biomass concentration in this setting.

In the previous settings, the decrease of light intensity only showed the decrease of growth rate and substrate consumption rate, however, in the 25% condition, it has shown that light is actually limiting the growth. This is confirmed by the substrate concentration change shown in figure 7. In figure 7 **a**, it can be seen that the acetate concentration gradually decreases but not as rapidly as it was in the previous three cases, where the concentration reached saturation even before the end of reaction phase. Here acetate is not limiting the growth as the full consumption of it is not observed within the reaction phase in any cycle of this setting. The same goes for ammonium and phosphate concentration as can be seen in figure 7 **b** and **c**, respectively, that their concentration does not reach a saturation point and keep decreasing till the end of reaction phase.

In the last setting of 25% light intensity, the removal ratio of ammonium and phosphate have further decreased to 15.89% and 13.44%. Biomass specific removal rate of acetate, ammonium and phosphate all have also decreased.

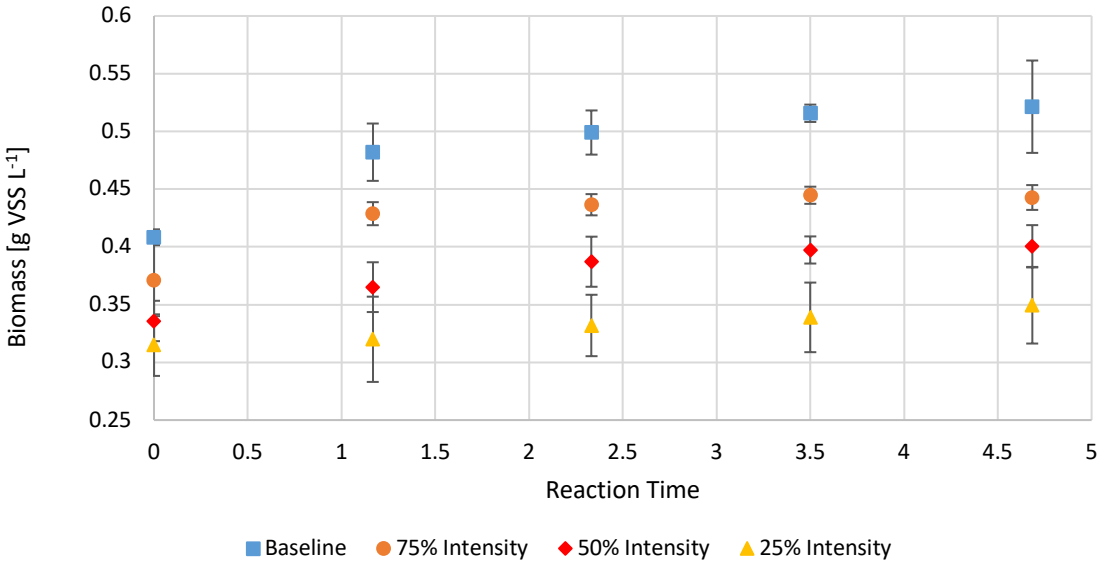

Figure 6. Biomass concentration change in four different light intensities; Baseline (350 W m^{-2}), 75% (262.5 W m^{-2}), 50% (175 W m^{-2}), and 25% (87.5 W m^{-2}). Concentrations of each point are average of 4 cycles except for the baseline case. Vertical bars indicate error rate of measurements from 4 cycles.

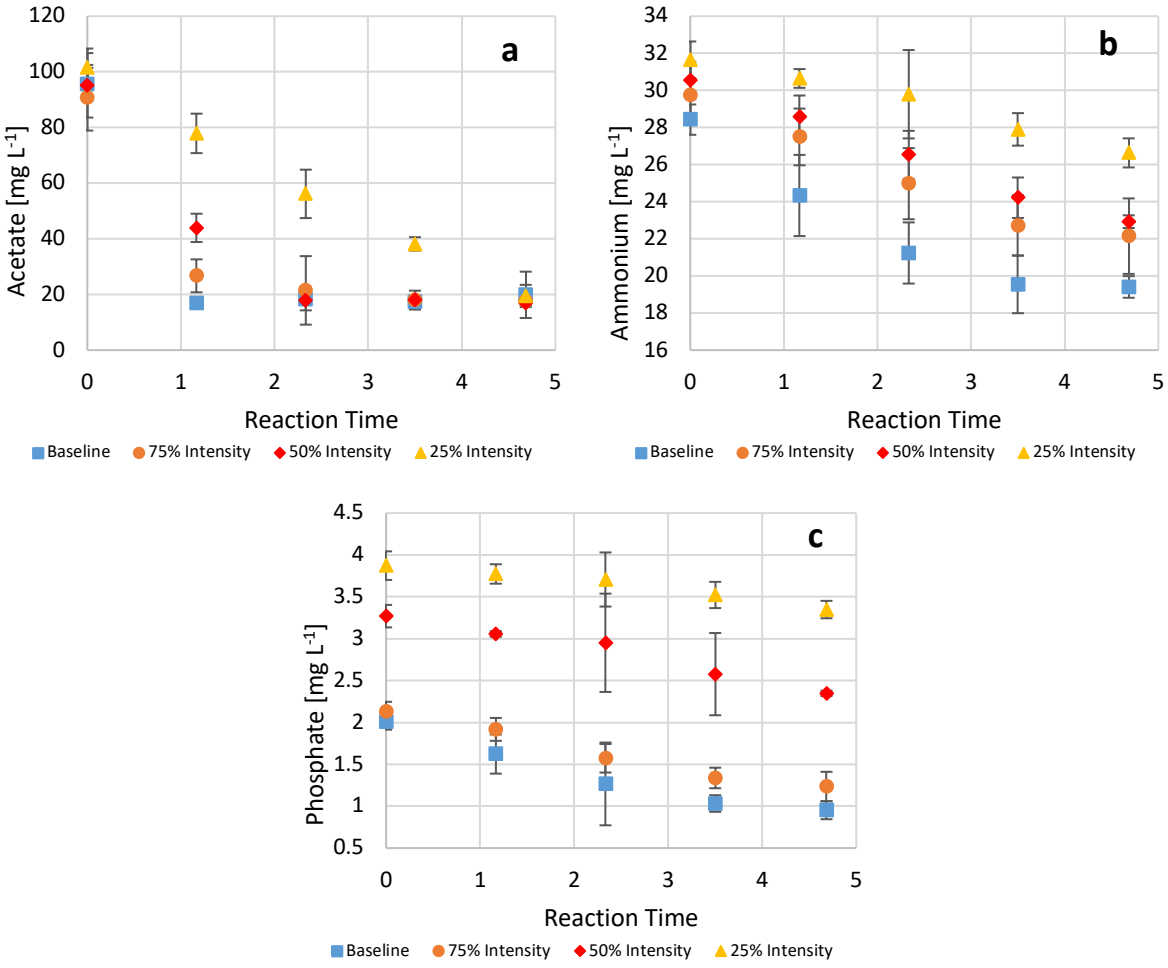

Figure 7. Nutrient removal trend of four different light intensities; Baseline (350 W m^{-2}), 75% (262.5 W m^{-2}), 50% (175 W m^{-2}), and 25% (87.5 W m^{-2}). Concentrations of each point are average of 4 cycles except for the baseline case. Vertical bars indicate error rate of measurements from 4 cycles. **a** Acetate, **b** Ammonium, **c** Phosphate

Table 2. Biomass and nutrient concentration comparison between different light conditions. Concentrations are average of 4 cycles except baseline condition which is of 3 cycles. Value inside bracket indicates standard deviation.

	Acetate [mg L^{-1}]			Ammonium [mg L^{-1}]		
Condition	Initial	Final	Removal Ratio [%]*	Initial	Final	Removal Ratio [%]*
Baseline	95.5 (3.0)	17.1 (0.3)	82.1	28.3 (0.4)	19.3 (0.5)	32.0
75% Intensity	90.7 (5.9)	17.8 (0.6)	80.4	29.8 (0.8)	22.1 (1.0)	25.6
50% Intensity	95.2 (5.8)	17.1 (0.5)	82.0	30.5 (0.5)	23.4 (1.0)	23.2
25% Intensity	101.5 (3.4)	19.5 (2.0)	80.8	31.7 (0.5)	26.6 (0.4)	15.9

	Phosphate [mg L^{-1}]			Biomass [mg L^{-1}]	
Condition	Initial	Final	Removal Ratio [%]*	Initial	Final
Baseline	2.0 (0.1)	1.0 (0.1)	52.3	412.1 (3.9)	538.5 (22.4)
75% Intensity	2.1 (0.1)	1.2 (0.1)	42.0	370.8 (17.5)	450.6 (6.0)
50% Intensity	3.3 (0.1)	2.4 (0.03)	27.2	331.1 (9.8)	403.1 (8.3)
25% Intensity	3.9 (0.2)	3.4 (0.1)	13.5	308.5 (14.8)	350.9 (16.7)

* Removal Ratio = (Initial – Final)/Initial x 100 [%]

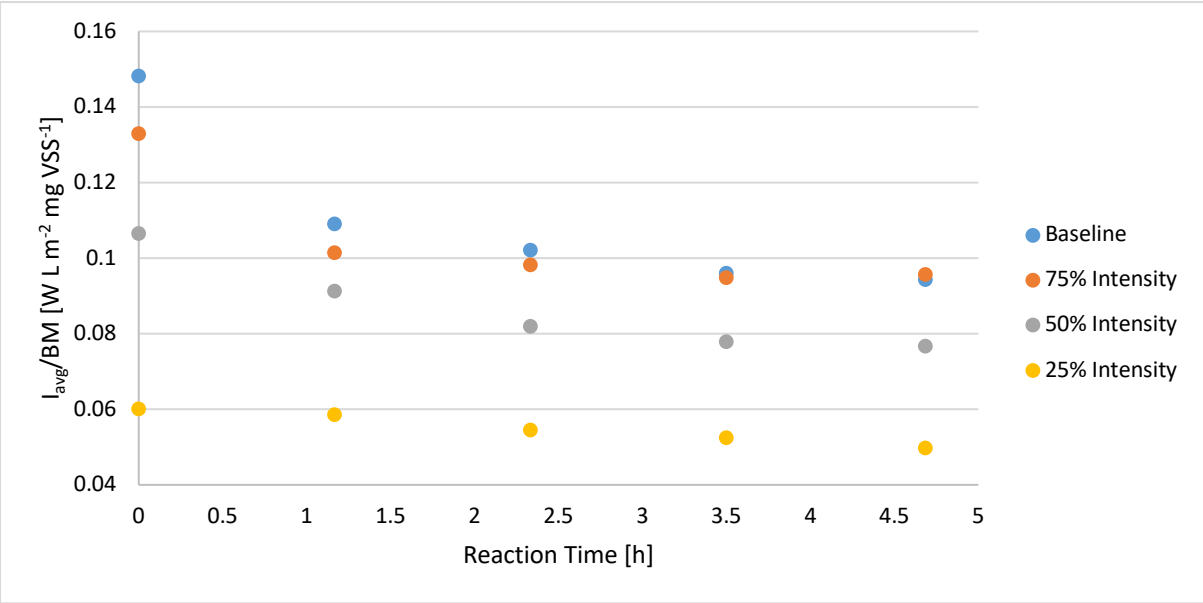

Figure 8. Biomass specific average light intensity ($\boldsymbol{I_{avg}/BM}$) change during reaction phase in the four settings. BM stands for biomass and $\boldsymbol{I_{avg}}$ is the average light intensity. Baseline (350 W m^{-2}), 75% intensity (262.5 W m^{-2}), 50% Intensity (175 W m^{-2}), 25% Intensity (87.5 W m^{-2})

The following two figures, figure 9 and figure 10, compare the initial biomass specific -growth rate and -uptake rate of substrates. From here on, unless mentioned, growth rate and removal/uptake rate are all referring to biomass specific initial rates. The values have been obtained from curve fitting with data obtained from wet lab experiments. It can be seen in figure 9 that the growth rate decreases as the light intensity decreases. Such decrease matches with the expectation that at higher light intensity, mixed culture PNSB will grow faster than in lower intensity cases when all other conditions remain the same. The ratio of growth rate of each condition to the baseline value does not strictly match with the light intensity ratio, which means the growth rate is not linearly proportional to the light intensity. From eq. (15), all other terms than light intensity can be neglected as it has been explained previously that light intensity is the growth rate-limiting factor. The equation 15 can be simplified as follows:

$$\mu = \mu_{max} \cdot \frac{S_I}{K_I + S_I}$$

Assuming that the μ_{max} value has not changed between each light condition, by lowering S_I value from that of baseline intensity to 25% intensity, the resulting μ ratio compared to baseline decreases from 96% (75% intensity) to 88% (50% intensity) and to finally 70% (25% intensity). This result shows that the assumption of equal μ_{max} is wrong and the μ_{max} value varies with changing light conditions. The change in μ_{max} can be interpreted as a change of population dynamics as all other conditions besides light hasn't changed. The change in population dynamics would also result in change of bulk biomass yield on substrates as the mixed culture

PNSB consists of wide genera of microorganisms and each has different biomass yield on acetate, ammonium, or phosphate. Thus, the acetate consumption rate is not linearly proportional to the light intensity. The acetate to biomass yields for the four intensity conditions are given in table 3 and the fluctuation of these values is most likely to be the result of microbial population dynamics. From the comparison of acetate removal rate, it can be seen that the uptake rate is highly influenced by light intensity.

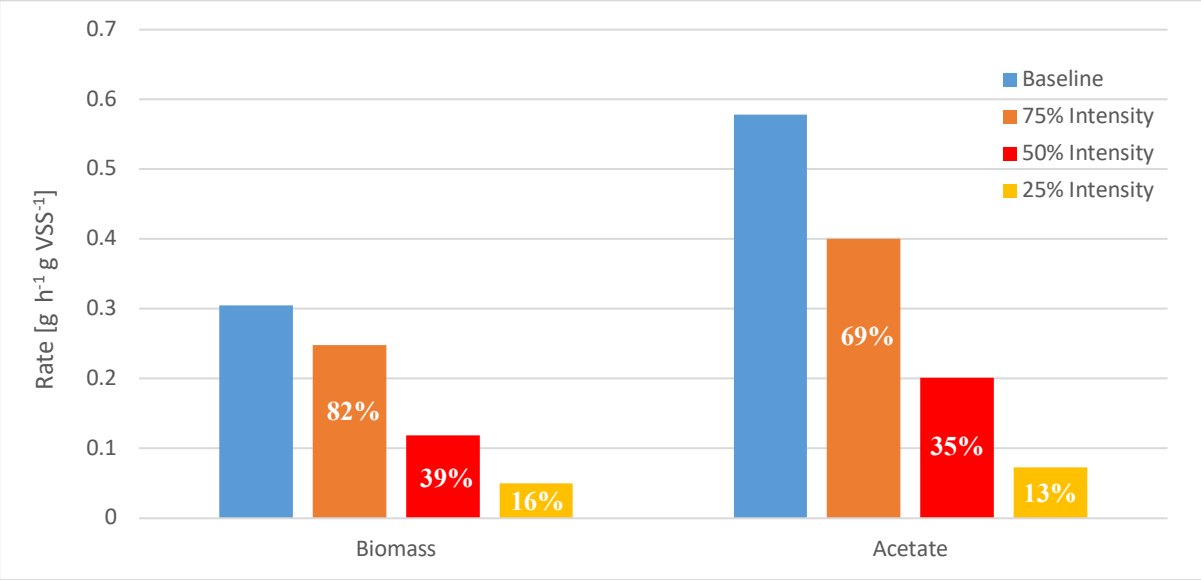

Figure 9. Comparison of initial biomass specific rate of biomass generation and acetate uptake of each setting. Rate is given as initial biomass specific rate. Percentage in the bar indicates the ratio of each value to baseline value. Baseline (350 W m^{-2}), 75% intensity (262.5 W m^{-2}), 50% Intensity (175 W m^{-2}), 25% Intensity (87.5 W m^{-2})

In figure 10, the other two nutrients' removal rates are shown. Ammonium uptake rate is also highly influenced by the light intensity just like acetate uptake rate. The ratio of ammonium uptake rate to biomass growth rate gives out the ammonium to biomass yield and the values for different light conditions are given in table 3. As it can be seen in table 3, the biomass yield on ammonium shows similar value in every condition. In the absence of nitrifiers, it is possible to say that all ammonium consumed is converted to biomass, and this full conversion leads to stable ammonium to biomass yield. From the microbial community composition result in figure 5, no known nitrifiers have been identified and since the system was maintained micro aerobic, the presence of nitrifiers can be neglected. This confirms the stable ammonium to biomass yield shown in table 3.

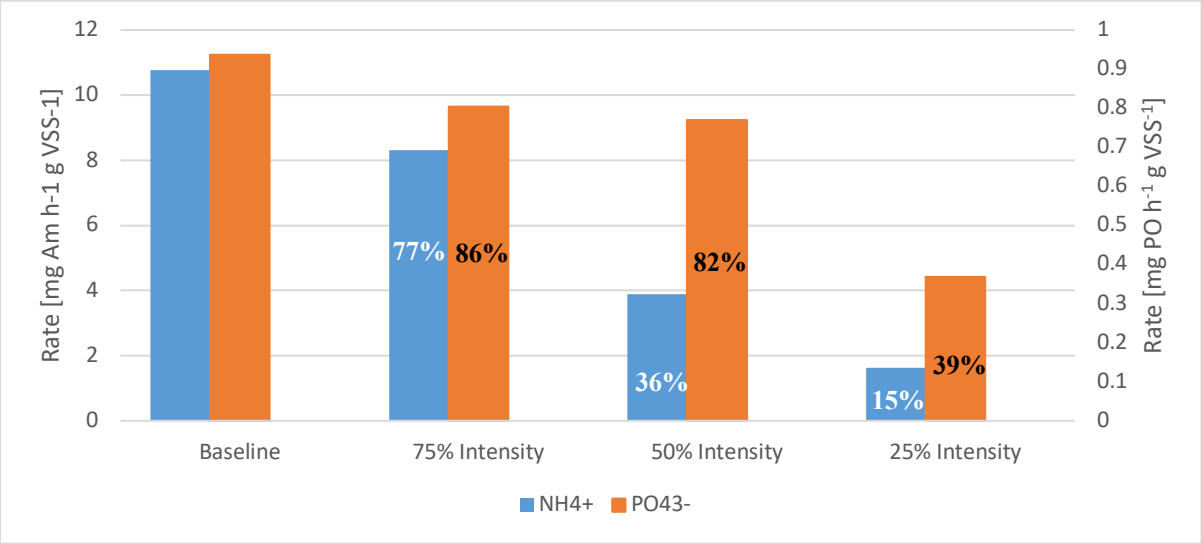

Figure 10. Comparison of initial biomass specific rate of ammonium (Am) and phosphate (PO) removal of each setting. Rate is given as initial biomass specific rate. Note that the unit of rate is given in mg h^{-1} $gVSS^{-1}$ compared to g h^{-1} $gVSS^{-1}$ in figure 8. Percentage in the bar indicate the ratio of each value to the baseline value. Baseline (350 W m^{-2}), 75% intensity (262.5 W m^{-2}), 50% Intensity (175 W m^{-2}), 25% Intensity (87.5 W m^{-2})

The relatively high acetate to biomass yield shows that the mixed culture would most likely be dominated by photoheterotrophs as their nature of metabolism allows them to fully utilize carbon sources in building up cell materials. The $Y_{X/S_{ac}}$ obtained in this study shows lower value than the reported value of 0.7 g VSS g Ac^{-1} for pure culture of *R. palustris* grown in an outdoor condition (Carlozzi & Sacchi, 2001) or 0.66 g VSS g Ac^{-1} for *R. palustris* (McKinlay & Harwood, 2010). The deviation in $Y_{X/S_{ac}}$ can be explained from the diversity of PNSB in the mixed culture with various $Y_{X/S_{ac}}$ values. The large decrease of $Y_{X/S_{PO}}$ between 75% intensity and 50% intensity indicates that there was a significant change in the population dynamics of the mixed culture. How the culture has changed and the change has influenced the $Y_{X/S_{PO}}$ values can't be answered at the moment with limited information of the culture composition. It might be possible that in higher light intensity conditions, the presence of phosphate accumulating organisms contributed to the high $Y_{X/S_{PO}}$ values.

Table 3. Biomass yield on each substrate at different light condition calculated by the ratio of initial biomass growth rate to initial substrate consumption rate. $\boldsymbol{Y_{X/S_{ac}}}$: Acetate to biomass yield, $\boldsymbol{Y_{X/S_{am}}}$: Ammonium to biomass yield, $\boldsymbol{Y_{X/S_{PO}}}$: Phosphate to biomass yield.

Condition	$Y_{X/S_{ac}}$ [g VSS g Ac^{-1}]	$Y_{X/S_{am}}$ [g VSS g Am^{-1}]	$Y_{X/S_{PO}}$ [g VSS g PO^{-1}]
Baseline	0.53	28.35	325.65
75% Intensity	0.62	29.83	308.28
50% Intensity	0.59	30.45	154.32
25% Intensity	0.69	30.79	135.79

In figure 11, the effect of average light intensity per biomass on the biomass specific growth rate is shown. The empirical equation in figure 11 shows that the growth rate will exponentially decrease as the average light intensity per biomass decreases and eventually reaches a non-zero value. This non-zero value is most likely to be coming from the non-phototrophic growth of the mixed culture PNSB. With figure 11, it is possible to identify among the substrates discussed (Acetate, Ammonium, Phosphate, and Light Intensity), which one is actually the growth rate-limiting substrate. As the figure indicates, growth rate increases as average light intensity increases. Since other conditions beside light intensity hasn't been changed, the increase of growth rate with increasing light intensity means that light is the growth rate-limiting factor; if light wasn't the limiting factor, growth rate will not change with increasing light intensity. If the light intensity further increases, it will eventually reach a certain point (saturation) where the increase of intensity does not change the growth rate any more unless other conditions change. The results of pure culture *Rps. spheroides* (Sistrom, 1962) and *Rps. capsulata* (Sojka & Gest, 1968) also shows that the biomass specific growth rate increases as light intensity increases and eventually shows a saturation.

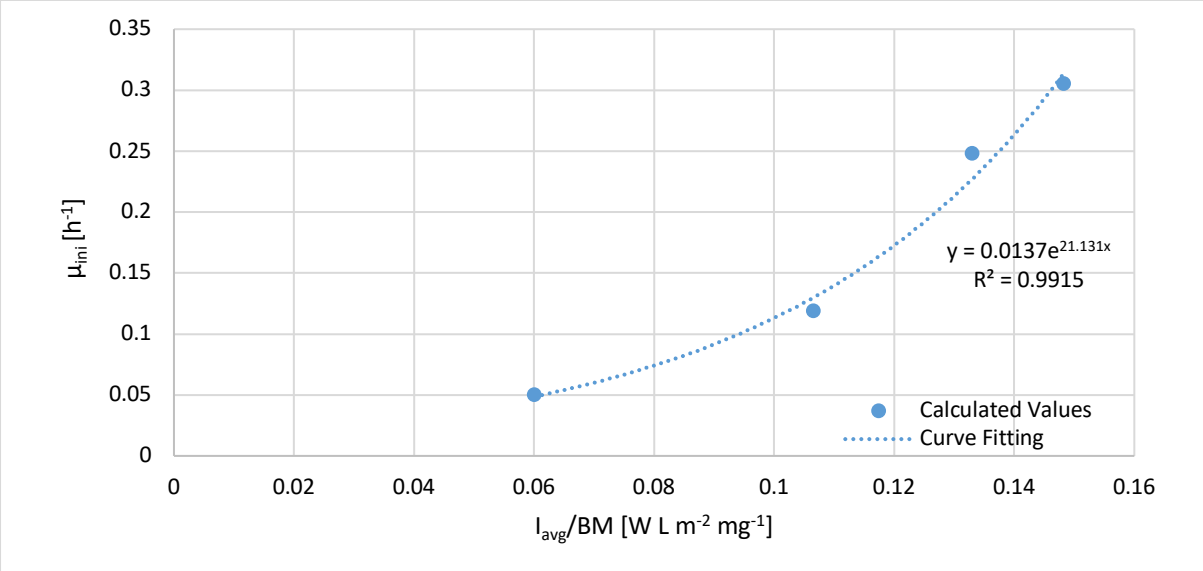

Figure 11. Biomass specific average light intensity ($\boldsymbol{I_{avg}/BM}$) versus initial biomass specific growth rate ($\boldsymbol{\mu_{ini}}$). The equation of the empirical model of this relationship was obtained by curve fitting.

In a batch cultivation of non-phototrophic organisms, the firstly depleted substrate is the growth-limiting substrate which controls both the growth yield and growth rate. However, for phototrophic organisms, the situation is more complicated as light is incorporated in the growth kinetics. Although light is significantly influencing the growth of phototrophs, it is only influencing the kinetic part of the growth but not on the stoichiometric part of it, since light is not a fixed matter but energy. The final biomass concentration is determined by the other

substrates (acetate, ammonium, phosphate, etc.) but not by the light intensity. In this sense, light intensity can only be said to limit the growth rate but not the growth yield.

While measuring the biochemical aspects of the culture, the physical characteristic in terms of settling rate of the biomass suspension was also measured. Comparing the settling rate does not directly show the density of the suspended biomass aggregates, but gives an indication of how the density changes with different light setting. The change of density can be translated to change of aggregate morphology, although, detailed explanation is not possible at the moment without any microscopic analyses. The following figure 12 shows the average settling rate of all 4 settings.

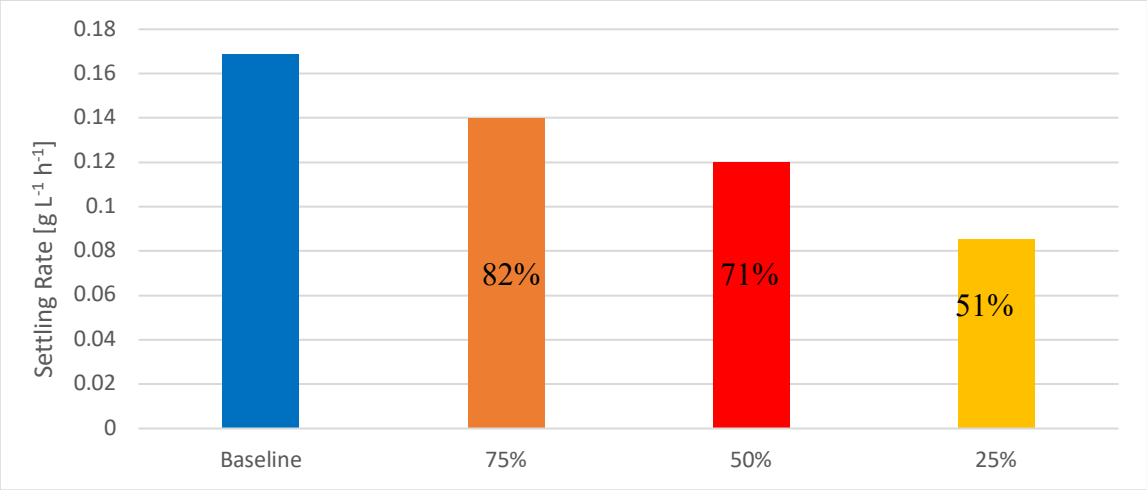

Figure 12. Settling rate change with different light settings. Intensity conditions are shown on the horizontal axis. Baseline (350 W m^{-2}), 75% intensity (262.5 W m^{-2}), 50% Intensity (175 W m^{-2}), 25% Intensity (87.5 W m^{-2}). Percentage in bar indicate ratio of settling rate at each setting to baseline settling rate.

As it can be seen from figure 12 the settling rate decreases as light intensity decreases. Higher settling rate literally means biomass is settling faster and hence, meaning their density is higher. This explains the decrease of initial biomass concentration along each setting, since after the settling phase, less biomass is remaining in the system at lower light intensity compared to higher intensity. In the first three settings where the initial acetate concentration is more or less the same and it is fully consumed before the end of reaction phase, which means growth is fully achieved before the end of reaction time, lower initial biomass concentration can only be explained by the loss of biomass after settling. In the last setting, both insufficient time for full growth and low settling rate lowers the initial biomass concentration. This is the reason why in the last setting, even between each cycle, initial biomass concentration decreases.

At the current stage of knowledge, it is impossible to clearly identify the reason why mixed culture PNSB forms denser biomass aggregates at higher light intensity. It is possible

that PNSB biomass produces more extracellular polymeric substances (EPS) that contribute to the formation of biomass aggregates. The effect of light intensity on the production of EPS has been shown to have a positive relationship in *Nostoc minitum*, a diazothophic cyanobacterium, (Pereyra & Ferrari, 2016) and in cyanobacterium *Arthrospira platensis* (Trabelsi, Ben Ouada, Bacha, & Ghoul, 2009). These results of these studies on cyanobacterium, however, can only give a rough guess for the production of EPS in mixed culture PNSB as they come from different phyla. Further studies on the EPS production related to light intensity change would answer why the density of biomass aggregates increase with increasing light intensity.

Comparison of wet-lab results with Aquasim simulation results

The simulation results of biomass growth and nutrient removal with *R. palustris* is shown in the following figures. In figure 13, the simulation result of biomass growth is compared with experimentally obtained results at different light intensity conditions. It can be seen from the figure 13 that the biomass concentration of *R. palustris* simulation shows lower saturation level in both baseline condition and 75% condition. The growth rates are faster in the experimental results than the simulation, as well as the final biomass concentration, even though the starting values are more or less the same. The large difference in final biomass concentration comes from deviation in biomass yield from substrates. The biomass yield of *R. palustris* on acetate is 0.665 g VSS g Ac^{-1} (McKinlay & Harwood, 2010) whereas that of the baseline and 75% were, based on mass balance but not by eq. (14), 1.61 g VSS g Ac^{-1} and 1.09 g VSS g Ac^{-1}, respectively. These significant gaps in biomass yield on acetate brought such difference in both consumption rate and final concentration.

The large deviation in μ_{ini} is the main reason for such difference in the shape of the growth curve. The baseline μ_{ini} has a value of 0.3 h^{-1} in experiment and that of simulation is only 0.057 h^{-1}, which is about 5 times smaller. The main reason for such small growth rate in simulation is coming from the fact that the μ_{max} value from literature (0.0825 h^{-1}) was obtained at lower light intensity condition; 60W light bulb was used in the study but not indicating the irradiance value (McKinlay & Harwood, 2010). This difference becomes smaller as the incident light intensity decreases to 25% condition where experimental value is 0.07 h^{-1} and the simulation is 0.038 h^{-1}. When compared to the results of Sojka and Gest (1968) on *Rhodopseudomonas capsulata* grown in batch operation with different light intensities, the experimentally obtained results show better similarity in growth rate, however, the comparison to the results of Sojka and Gest should be taken with care as their measurement of light intensity

is in ft-c unit but not in W m^{-2} unit and D-malate was used as carbon source instead of acetate. The conversion of ft-c to W m^{-2} is strongly dependent on the light source used, and thus needs special care. Nevertheless, rough comparison can be made with some assumption on the light source. Assuming the light source used in their case, Lumiline lamp, is identical to fluorescent lamp, the resulting growth rates are 0.38 h^{-1} (430 W m^{-2}), 0.35 h^{-1} (287 W m^{-2}), 0.28 h^{-1} (144 W m^{-2}), and 0.1h^{-1} (36 W m^{-2}); intensity inside brackets are incident intensity. Even though they used different carbon source for growth, the rates at higher light intensity are more similar than compared to that of McKinlay and Harwood (2010). It is still of doubt whether the change of carbon source would result in such huge difference of growth rate and further research needs to be done.

Figures 14 and 15 show comparison of simulation and experimental results of acetate and ammonium, respectively. In the simulation, unlike the experimental results, acetate is fully consumed to almost zero concentration. This difference in final concentrations could mean that the mixed culture PNSB is experiencing a growth limitation other than the measured substrates that would stop the consumption of acetate, or could indicate that there is a sort of threshold concentration that they can uptake. Another possibility is that, as mentioned above, the acetate concentration of samples at the saturation points were very close to the detection limit of the HPLC system used so that the resulting concentrations contained significant error. For ammonium, the simulation shows better removal with slightly faster consumption in both conditions. In the simulation the plateau can be observed better than the experimental results which is the consequence of acetate limitation in growth. As acetate is fully consumed by the biomass in simulation results, ammonium consumption fully stops, whereas in the experimental results, it can be seen that the ammonium is still consumed after the acetate concentration reaches the plateau. To explain this mismatch in substrate consumption pattern, more investigation is necessary.

In 50% condition, the simulation of biomass concentration shows less deviation with the experimental results than the previous two conditions. Final biomass concentration has a deviation of only 4.4% with experimental result. As the final biomass concentration is more or less the same and the initial substrate concentrations are also the same, the main reason why the simulation result shows slower growth rate is due to different half saturation constants. Biomass yield on substrates have no influence on the biomass growth rate as it can be found from eq.(15); no yield term exists in the rate equation. Acetate and ammonium still show deviation in both consumption rate and final concentration as before and the reason is a combined effect of mainly different biomass yield on substrates and μ_{max}.

In the 25% light intensity condition, the simulation shows better performances in all rates and final concentrations. The biomass yield on acetate calculated with mass balance in 25% intensity condition is 0.52 g VSS g Ac^{-1} which is a lower value than that of *R.palustris*. The higher biomass yield of simulation resulted in higher final concentration shown in figure 13 c. From the simulation results, the biomass specific growth rate for each light condition are 0.057 h^{-1}, 0.055 h^{-1}, 0.05 h^{-1}, and 0.04 h^{-1}, respectively. This decline in growth rate is a certain indication that the light intensities studied here fall into the region where light is limiting the

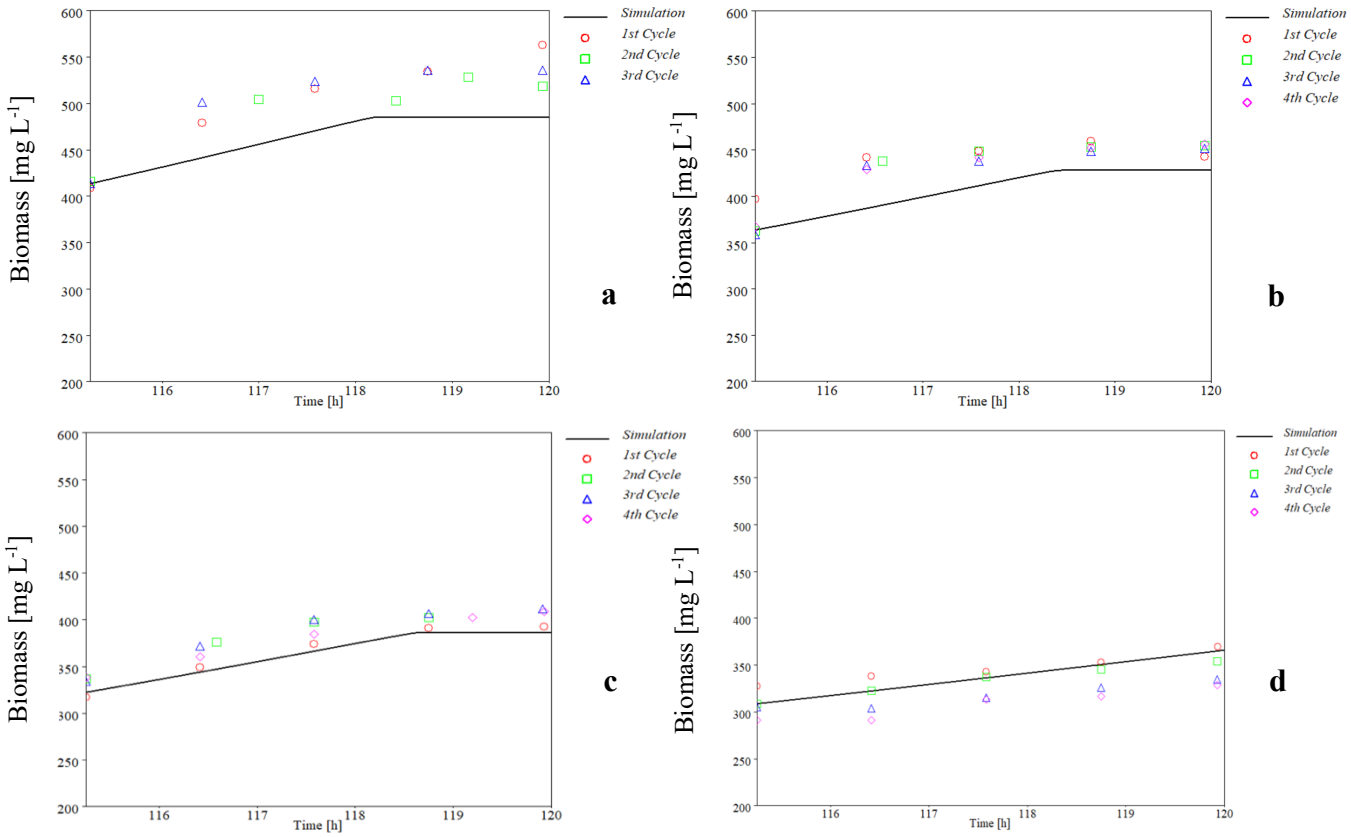

Figure 13. Comparison of biomass growth simulation and wet-lab results at different light intensity conditions in reaction phase. **a** Baseline; **b** 75% Intensity; **c** 50% Intensity; **d** 25% Intensity. Time scales are different since the simulation was run until the results showed an equilibrium state.

growth rate.

The faster growth and better nutrient removal rate in mixed culture PNSB would eliminate the necessity to obtain and maintain a pure culture of PNSB in wastewater treatment plant. The unnecessity of obtaining and maintaining a pure culture of PNSB would be of great advantage for an operator in both the performance and cost wise. The process control to maintain a stable and pure culture needs more care as unpredictable factors can severely affect the population dynamics, whereas in mixed culture PNSB, the control of population dynamics would be relatively easier as introduction of alien organism is not of an important concern.

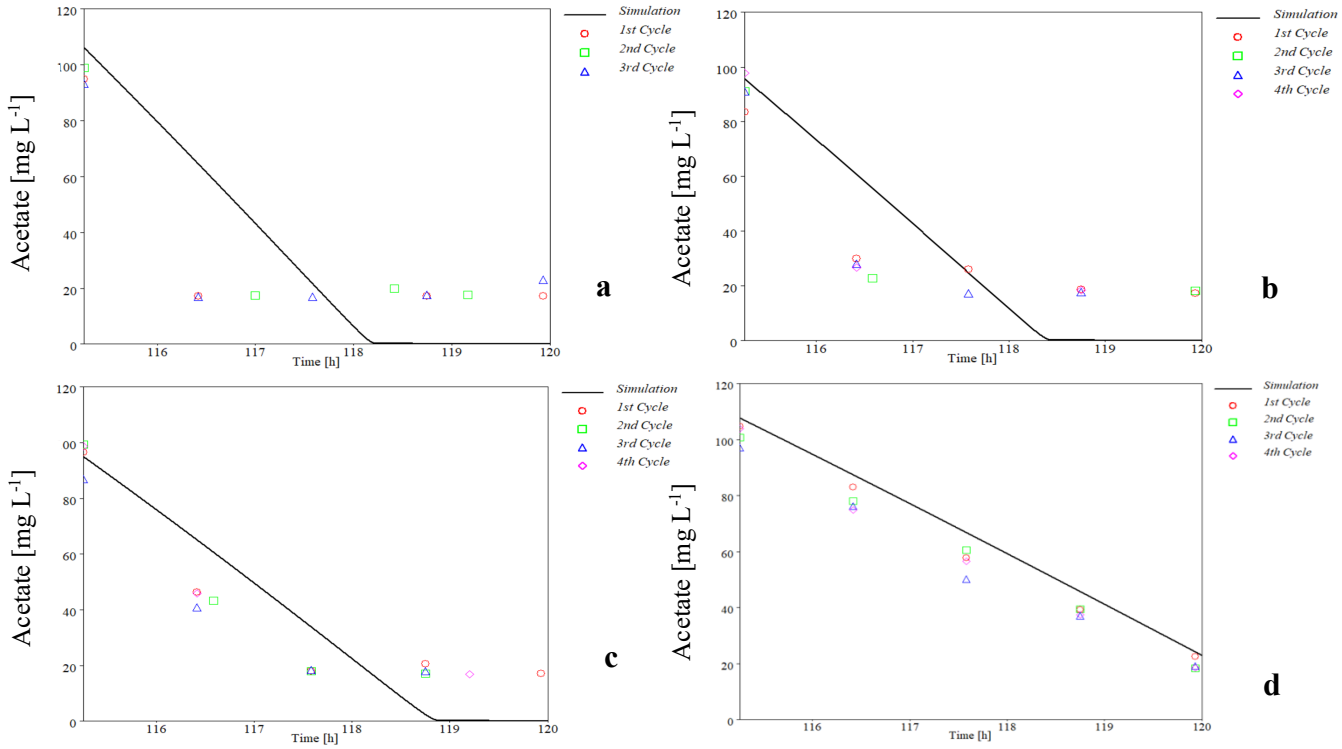

Figure 14. Comparison of acetate removal simulation and wet-lab results at different light intensity conditions in reaction phase. **a** Baseline; **b** 75% Intensity; **c** 50% Intensity; **d** 25% Intensity. Time scales are different since the simulation was run until the results showed an equilibrium state.

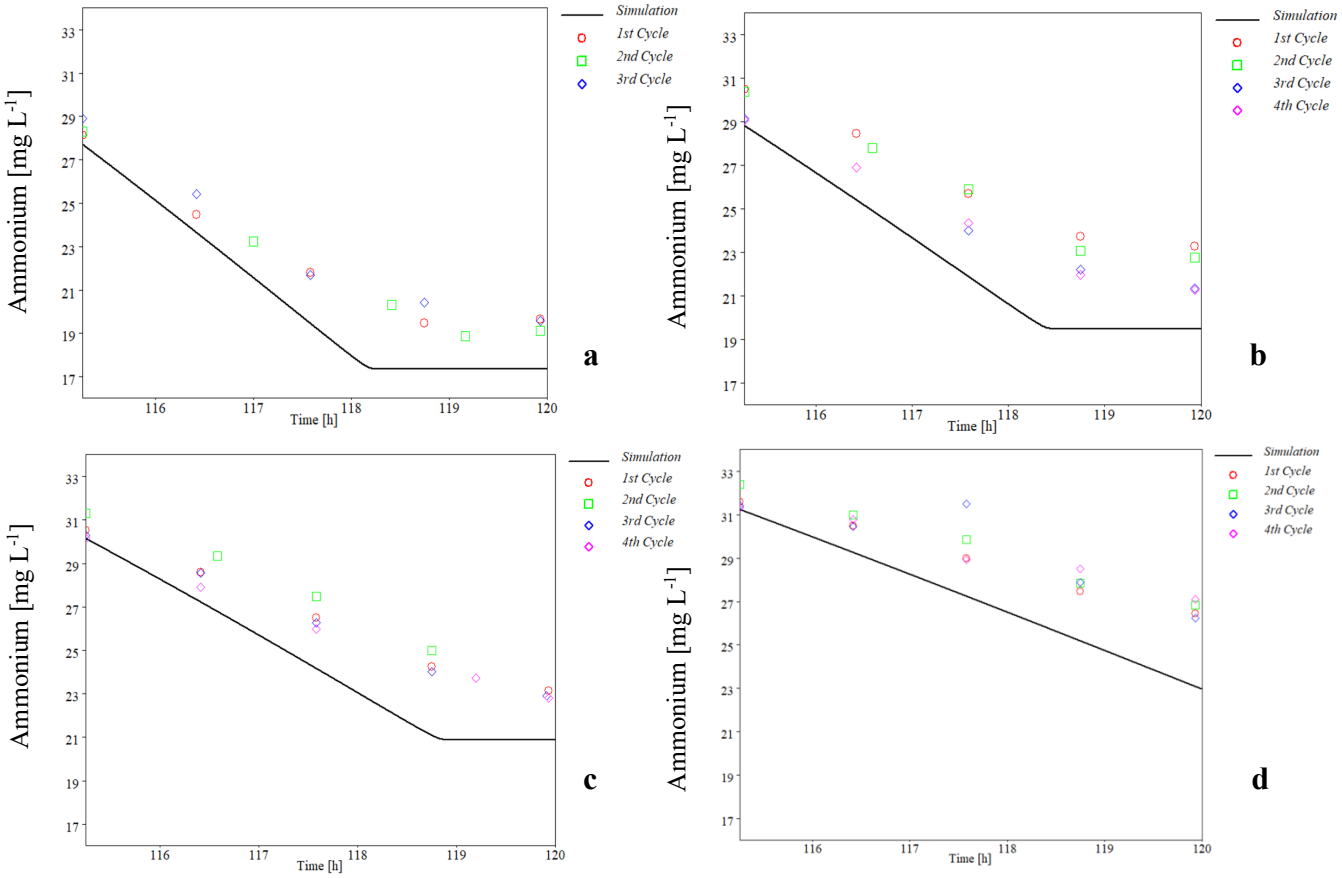

Figure 15. Comparison of ammonium removal simulation and wet-lab results at different light intensity conditions in reaction phase. **a** Baseline; **b** 75% Intensity; **c** 50% Intensity; **d** 25% Intensity. Time scales are different since the simulation was run until the results showed an equilibrium state.

3.2.2. Photo-pigment Content Change with Different Light Intensity

Prior to directly investigating the photo-pigment content of each sample, methods for photo-pigments extraction was validated. In figure 16, the spectral scan results of crude extracts assisted with various sonication settings are shown. The result without sonication shows relatively lower absorbance value in the peak at 770 nm, wavelength which corresponds to the maximum peak of bacteriochlorophyll a in the acetone/methanol extract solvent. Samples used for the comparison of extraction methods had the same biomass concentration and were examined with the same measuring volume of 200 µL, and thus, absorbance is directly proportional to the concentration of bacteriochlorophyll. Other small peaks at 445 nm, 475 nm and 502 nm indicate different types of unidentified carotenoids. Since the mixed culture consists of wide variety of genera and species of PNSB, the total bacteriochlorophyll a content can't be obtained from the bulk cells directly and can only be obtained after extraction.

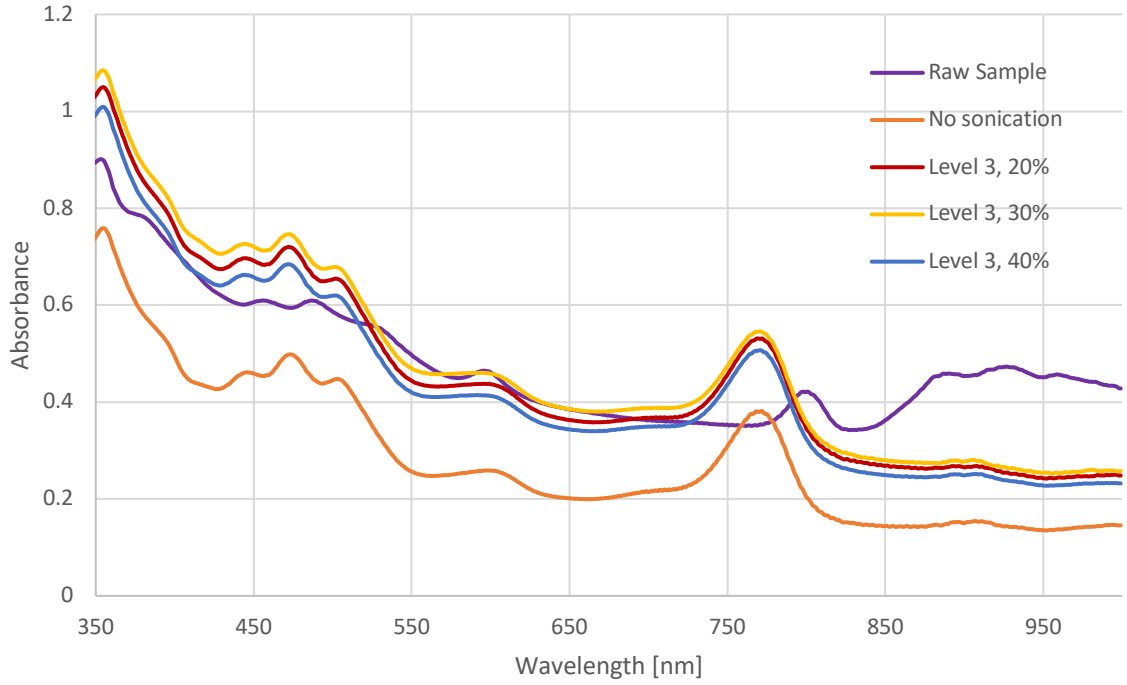

Figure 16. Spectral scan comparison between different sonication settings. Raw sample: Biomass sample in demineralized water, No sonication: Biomass sample in extraction solvent, Level 3: output setting of sonicator used which corresponds to 20W, percentages are proportions of sonication time to total operation time. Higher output settings were not chosen as they caused heating of the extracts and overloading out of the sample container. Lower output settings were also not chosen as they would obviously show lower performance in cell disruption.

Bacteriochlorophyll a content in biomass was calculated by dividing the bacteriochlorophyll a concentration in the crude extract with the biomass concentration. This pigment content is expected to remain constant within a cycle but may vary slightly between each cycle due to minor alteration in the culture population.

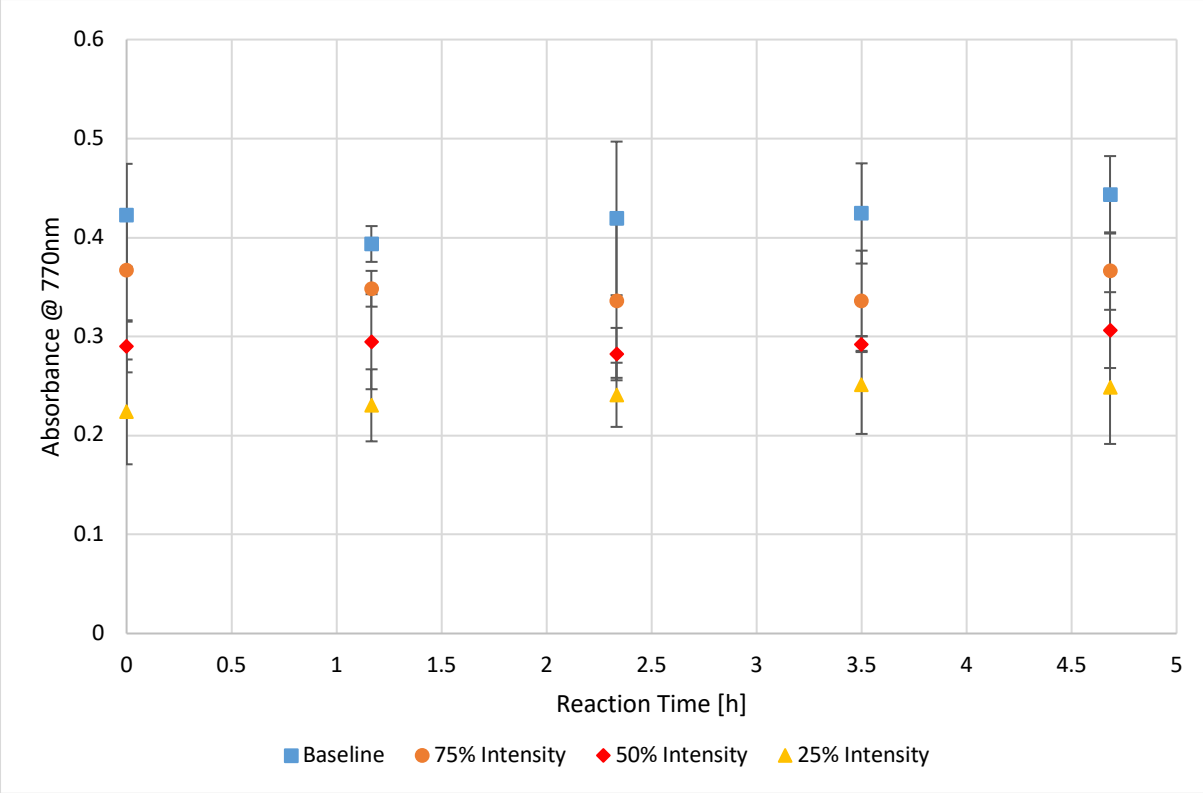

Figure 17. Absorbance change of raw pigment extract of 4 light conditions in reaction phase measured with plate reader. Absorbance at 770nm corresponds to maximum absorbance peak of bacteriochlorphyll. Bars in each point indicate error rate. Baseline (350 W m^{-2}), 75% intensity (262.5 W m^{-2}), 50% Intensity (175 W m^{-2}), 25% Intensity (87.5 W m^{-2})

In figure 17, the absorbance data within each condition does not show an increasing trend as expected; photo-pigment concentration in extract is expected to increase with biomass concentration. Also, the results show large error in their measurement and the reason for such deviation is due to the strong influence of path length in converting absorbance to concentration. It was impossible to directly measure the path length of each sample in the well plate because the path length measurement option of the plate reader was only available for aqueous solutions, but not the solvent used for extraction. In order to solve this issue, a simple assumption was made that the path length for 200 µL of extraction solvent is the same as that of 200 µL of water. However, as the absorbance result in figure 17 shows, such assumption of using equal path length turned out to be inappropriate.

As it can be seen in the figure 18, the bacteriochlorphyll content between each cycle in the same setting does not remain strictly constant. This is most likely coming from the change in microbial culture composition between each cycle and the error in converting absorbance to bacteriochlorophyll concentration mentioned above. The setting average increases from baseline setting to 75% condition, and then decreases to 25% condition. The increase of bacteriochlorphyll content from baseline condition to 75% condition is logical as more photo-pigments are required for phototrophs to gain enough light energy for growth. However, the

decrease after 75% condition does not match with expectation that pigment content increases with decreasing light intensity (Cohen-Bazire et al., 1957). The reason for decrease in bacteriochlorophyll content can be explained with changing PNSB proportion in the mixed culture. At the current stage it is only possible to presume that the reason for such change is due to the population change.

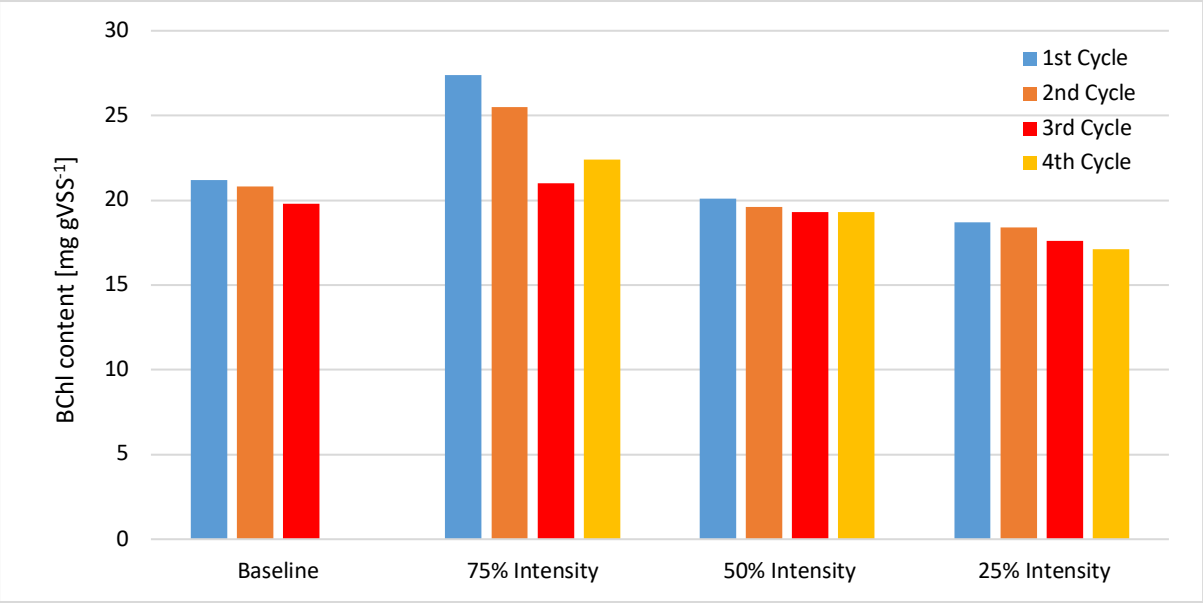

Figure 18. Bacteriochlorophyll (Bchl) content obtained from micro well plate reading of biomass in different light settings. Baseline (350 W m^{-2}), 75% intensity (262.5 W m^{-2}), 50% Intensity (175 W m^{-2}), 25% Intensity (87.5 W m^{-2})

As a comparison to the well plate reader, RP-HPLC system was also used to identify bacteriochlorophyll content in the biomass. Prior to analyzing the samples, calibration of bacteriochlorophyll was performed and the result can be seen in the appendix. The conversion of peak area to bacteriochlorophyll concentration at low concentration showed significant errors in both 363 nm and 270 nm. Although the calibration curve in appendix showed a high R^2 value, the standard concentrations used for calibration was too high compared to detected bacteriochlorophyll concentration from the samples. At the lowest concentration used in calibration, 83 mg L^{-1}, the error rate between standard concentration and the concentration calculated from peak area with calibration curve was 37.8% for 270 nm and 17.6% for 363 nm.

The result of RP-HPLC is shown in figure 19. As it can be seen in figure 19, the bacteriochlorophyll content measured with 270 nm shows much higher value than that measured with 363 nm. This huge difference mainly comes from the integration error of the peak signal in the detector and the conversion of peak area to bacteriochlorophyll concentration. As explained above, the error rates in conversion of peak area to concentration are significantly large that the converted concentrations were overestimated to more than 37.8% for 270 nm and 17.6% for 363 nm. The higher conversion error in 270 nm makes such

huge difference in bacteriochlorophyll content values shown in figure 19. Moreover, in some cases, manual integration of peaks had to be done because of false integration and this has also significantly contributed on resulting such huge difference in bacteriochlorophyll content between the two monitored wavelengths.

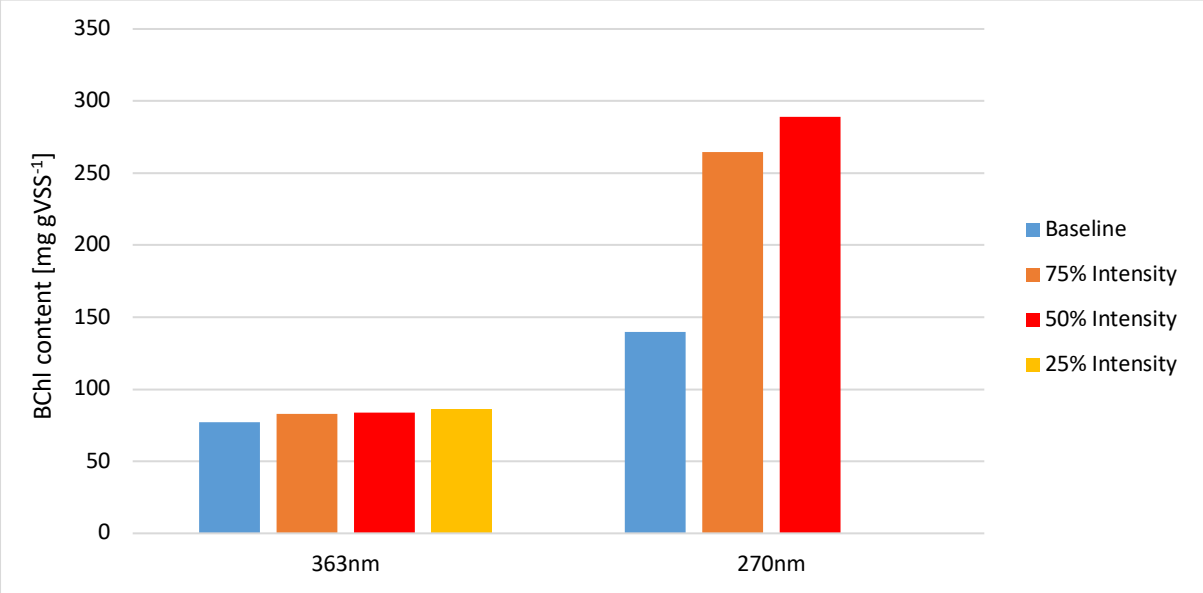

Figure 19. Bacteriochlorophyll (BChl) content in different settings obtained with RP-HPLC. Wavelength in horizontal axes stands for monitored wavelength in the PDA detector of the RP-HPLC system. In 270nm, 25% intensity result is missing because the concentration of BChl in the samples were below detection limit. Baseline (350 W m^{-2}), 75% intensity (262.5 W m^{-2}), 50% Intensity (175 W m^{-2}), 25% Intensity (87.5 W m^{-2})

The results of micro well plate readings and the RP-HPLC results, show huge difference in bacteriochlorophyll content. Microbial population information is necessary to confirm which of these three results is most reliable. The increase of bacteriochlorophyll content in the first two light settings is universal in all three analysis results. However, the content change after 75% light intensity condition shows huge variation between each other as in plate reader, the content decreases, in 363 nm readings it remains more or less the same, and in 270 nm readings it increases. The culture configuration information will provide useful information to quantitatively compare the three analysis results after 75% light intensity and finally validate of which three analysis results is the most reliable. With the current stage of knowledge, it is impossible to make conclusions about these results.

3.2.3. General discussion of light intensity effect on mixed culture PNSB

It was found that the light intensity change has significant effect on the growth rate and nutrients removal rate of PNSB in mixed culture. It was found out that the growth rate has strong dependence on light intensity, and this highlights the importance of light energy in photoheterotrophic growth. As light intensity decreased, growth rate decreased to 16% of its original at the lowest intensity (87.5W m^{-2}) applied. The decrease of growth rate with declining light intensity has further diminished the nutrient removal rate; strongest influence on acetate consumption rate. This relationship of light intensity with biomass growth rate would allow further researchers to find an optimum point where, in the purpose of nutrient removal, the most energy efficient nutrient removal can be obtained. The results of this study did not fully answer the question arose in section 1.3., as the light saturation level had not been identified. Nevertheless, the strong dependency of light intensity on growth rate and nutrient removal rate had been identified. For the question regarding photo-pigment content, as the results showed, neither quantitative nor qualitative interpretation was possible.

The SBR operation of mixed culture PNSB at high intensity allowed biomass to form denser aggregates than in lower light intensity, and this information would be of importance for further research on the implication of mixed culture PNSB on SBR at different scale. This relationship between biomass aggregate density and light intensity would be of critical importance for the operation of a mixed culture PNSB reactor for the prevention of biomass washout. By controlling the light intensity, it would be possible to control the SRT instead of controlling the SRT by the hydraulic retention time (HRT), however, further studies are required to verify whether this option is possible and reasonable.

4. Conclusion

The effect of light intensity on the growth and nutrient removal of mixed culture PNSB was studied and as postulated in the hypothesis section, growth rate and nutrient removal rates were diminished as incident light intensity decreased. However, it was impossible to identify the saturation level of light intensity and the presence of photo-inhibition level. Nonetheless, with the given media composition, the light intensity of operated showed growth rate-limitation. To overcome the limitation, it would be possible to either increase the incident light intensity or decrease the biomass concentration so that the I_{avg}/BM value increases above the rate-limitation level.

Direct comparison with published works always showed difficulty as the culture studied in this report consisted of wide genera of PNSB and even other organisms. Moreover, the variation in used light source and measured light intensity in different units severed the complexity of direct comparison to obtain useful information.

Additionally, it was not possible to precisely quantify the effect of light intensity change on the bacteriochlorophyll content of mixed culture PNSB. Qualitative comparison would be available in the presence of microbial community information at different light intensity conditions.

The five key take-home messages from this study include:

1. Decrease of light intensity has diminished the growth rates of PNSB in the mixed culture by 82% (75% Intensity), 39% (50% Intensity) and 16% (25% Intensity).
2. Operated light intensities with the given medium were in the range of growth rate-limiting range
3. Change of light intensity has changed the characteristics of the cell aggregates. At lower light intensity, the PNSB based biomass tends to forms less dense cell aggregates than at higher intensity and thus have lower settling rate of 82% (75% Intensity), 71% (50% Intensity), and 51% (25% Intensity) compared to baseline settling rate
4. Extraction process of bacteriochlorophyll was validated and the process assisted with sonication showed superior results than no assistance.
5. Microwell plate analysis of bacteriochlorophyll may not be appropriate even though its strength of high throughput and accuracy in measurement for the high uncertainty in

sample preparation. RP-HPLC analysis of bacteriochlorophyll needs further optimization as the inconsistency of results indicate

Overall, this study revealed important information on the response of mixed culture PNSB's response to altering light intensity. Then, the necessity of further investigation arises for both application aspects and academic aspects of mixed culture PNSB.

5. Outlook and Recommendations

Complete information on population dynamics of four conditions would provide more information on the response of mixed culture PNSB to different light intensity. With more extreme cases of light intensity settings, it would also be possible to observe the light inhibition of PNSB growth and provide useful information on the operation window of light intensity. The change in settling rate was of something not expected, and more research is necessary to identify why such variation of biomass aggregate density happens with different light intensity.

The calculation of average light intensity in the photo-bioreactor uses some approximations. It is calculating the available light intensity for phototrophs; however, phototrophs can't utilize this available light fully as the nature of light does not allow this. In order to precisely calculate, or measure, the light energy that has been utilized by phototrophs, it is better to use utilized light rather than available light. Utilized light would be the remaining light after non-absorption processes in the attenuation of light. For this, further studies on the scattering of light with mixed culture PNSB would be necessary to obtain the purely absorbed light by PNSB. Moreover, the attenuation model developed in this study needs to be verified as well with experimentally obtained values. For this, a waterproof photosensor unit should be installed to the reactor to obtain the light attenuation profile.

The quantification process of bacteriochlorophyll with micro plate reader should substituted with spectrophotometer using standardized cuvettes as vessels. The uncertainty in path length measurements highly influences the bacteriochlorophyll content calculation. The use of spectrophotometer will give out more robust results with less measurement error as they use standardized cuvettes of 1cm path length. The absence of path length correction in the spectrophotometer measurement will significantly lower the measurement error.

The sample preparation of RP-HPLC should also be optimized as the results of it showed enormous error incorporated in the conversion of peak area to concentration, especially at lower pigment concentration. The volume of extraction solvent could be reduced to manually increase the pigment concentration to above a concentration where the error rate is relatively lower. Increasing the injection volume of sample in the RP-HPLC system may not be favorable as it increases the risk of signal peak broadening in the detector.

Bibliography

Adessi, A., & De Philippis, R. (2014). Photobioreactor design and illumination systems for H_2 production with anoxygenic photosynthetic bacteria: A review. *International Journal of Hydrogen Energy*, *39*(7), 3127–3141. https://doi.org/10.1016/j.ijhydene.2013.12.084

Aiking, H., & Sojka, G. (1979). Response of *Rhodopseudomonas capsulata* to illumination and growth rate in a light-limited continuous culture. *Journal of Bacteriology*, *139*(2), 530–536. Retrieved from http://www.ncbi.nlm.nih.gov/pubmed/457612

Akkerman, I., Janssen, M., Rocha, J., & Wijffels, R. H. (2002). Photobiological hydrogen production: Photochemical efficiency and bioreactor design. *International Journal of Hydrogen Energy*, *27*(11–12), 1195–1208. https://doi.org/10.1016/S0360-3199(02)00071-X

Androga, D. D., Özgür, E., Eroglu, I., Gündüz, U., & Yücel, M. (2012). Photofermentative hydrogen production in outdoor conditions. *Hydrogen Energy - Challenges and Perspectives*, (May 2014), 77–120. https://doi.org/10.5772/50390

Brune, D. C. (1995). Sulfur compounds as photosynthetic electron donors. In B. C. E. Blankenship R.E., Madigan M.T. (Ed.), *Anoxygenic Photosynthetic Bacteria* (pp. 847–870). Dordrecht: Kluwer Academic Publishers. https://doi.org/10.1007/0-306-47954-0_39

Carlozzi, P., Pushparaj, B., Degl'Innocenti, A., & Capperucci, A. (2006). Growth characteristics of *Rhodopseudomonas palustris* cultured outdoors, in an underwater tubular photobioreactor, and investigation on photosynthetic efficiency. *Applied Microbiology and Biotechnology*, *73*(4), 789–795. https://doi.org/10.1007/s00253-006-0550-z

Carlozzi, P., & Sacchi, A. (2001). Biomass production and studies on *Rhodopseudomonas palustris* grown in an outdoor, temperature controlled, underwater tubular photobioreactor. *Journal of Biotechnology*, *88*(3), 239–249. https://doi.org/10.1016/S0168-1656(01)00280-2

Codgell, R. J., Southall, J., Gardiner, A. T., Law, C. J., Gall, A., Roszak, A. W., & Isaacs, N. W. (2006). How purple photosynthetic bacteria harvest solar energy. *Comptes Rendus Chimie*. https://doi.org/10.1016/j.crci.2005.03.035

Cogdell, R. J., Howard, T. D., Bittl, R., Schlodder, E., Geisenheimer, I., Lubitz, W., … Buc, C. (2000). How carotenoids protect bacterial photosynthesis. In *Philosophical Transactions of the Royal Society B: Biological Sciences* (Vol. 355, pp. 1345–1349).

https://doi.org/10.1098/rstb.2000.0696

Cohen-Bazire, G., Sistrom, W. R., & Stanier, R. Y. (1957). Kinetic studies of pigment synthesis by non-sulfur purple bacteria. *Journal of Cellular and Comparative Physiology*, *49*(1), 25–68. https://doi.org/10.1002/jcp.1030490104

Cooper, D. E., Rands, M. B., & Woo, C.-P. (1975). Sulfide reduction in fellmongery effluent by red sulfur bacteria. *Journal (Water Pollution Control Federation)*, *47*(8), 2088–2100. Retrieved from http://www.jstor.org/stable/25038944

Cornet, J.-F., & Albiol, J. (2000). Modeling photoheterotrophic growth kinetics of *Rhodospirillum rubrum* in rectangular photobioreactors. *Biotechnology Progress*, *16*(2), 199–207. https://doi.org/10.1021/bp990148q

Frigaard, N.-U., Takaichi, S., Hirota, M., Shimada, K., & Matsuura, K. (1997). Quinones in chlorosomes of green sulfur bacteria and their role in the redox-dependent fluorescence studied in chlorosome-like bacteriochlorophyll c aggregates. *Archives of Microbiology*, *167*(6), 343–349. https://doi.org/10.1007/s002030050453

Gest, H., Kamen, M. D., & Bregoff, H. M. (1950). Studies on the metabolism of photosynthetic bacteria: v. Photoproduction of hydrogen and nitrogen fixation by *Rhodospirillum rubrum*. *The Journal of Biological Chemistry*, *182*(1), 153–170.

Hansen, T. A., & van Gemerden, H. (1972). Sulfide utilization by purple nonsulfur bacteria. *Archiv Für Mikrobiologie*, *86*(1), 49–56. https://doi.org/10.1007/BF00412399

Harwood, C. S., & Gibson, J. (1988). Anaerobic and aerobic metabolism of diverse aromatic compounds by the photosynthetic bacterium *Rhodopseudomonas palustris*. *Appl Environ Microbiol*, *54*(3), 712–717.

Hiraishi, A., Shi, J.-L., & Kitamura, H. (1989). Effects of organic nutrient strength on the purple nonsulfur bacterial content and metabolic activity of photosynthetic sludge for wastewater treatment. *Journal of Fermentation and Bioengineering*, *68*(4), 269–276. https://doi.org/10.1016/0922-338X(89)90028-7

Hülsen, T., Batstone, D. J., & Keller, J. (2014). Phototrophic bacteria for nutrient recovery from domestic wastewater. *Water Research*, *50*(0), 18–26. https://doi.org/10.1016/j.watres.2013.10.051

Katsuda, T., Fujii, N., Takata, N., Ooshima, H., & Katoh, S. (2002). Light attenuation in suspension of the purple bacterium *Rhodobacter capsulatus* and the green alga *Chlamydomonas reinhardtii*. *Journal of Chemical Engineering of Japan*, *35*(5), 428–435. https://doi.org/10.1252/jcej.35.428

Levin, D. B., Pitt, L., & Love, M. (2004). Biohydrogen production: Prospects and limitations

to practical application. *International Journal of Hydrogen Energy*, *29*(2), 173–185. https://doi.org/10.1016/S0360-3199(03)00094-6

Liao, Q., Wang, Y. J., Wang, Y. Z., Zhu, X., Tian, X., & Li, J. (2010). Formation and hydrogen production of photosynthetic bacterial biofilm under various illumination conditions. *Bioresource Technology*, *101*(14), 5315–5324. https://doi.org/10.1016/j.biortech.2010.02.019

Lodish, H., Berk, A., Kaiser, C. A., Krieger, M., Bretscher, A., Ploegh, H., … Martin, K. C. (2016). *Molecular Cell Biology* (8th ed.). New York: W. H. Freeman and Company.

Madigan, M. T., & Jung, D. O. (2009). An overview of purple bacteria: systematics, physiology, and habitats. In C. N. Hunter, F. Daldal, M. C. Thurnauer, & J. T. Beatty (Eds.), *The Purple Phototrophic Bacteria* (pp. 1–15). Dordrecht: Springer Netherlands. https://doi.org/10.1007/978-1-4020-8815-5_1

McKinlay, J. B., & Harwood, C. S. (2010). Carbon dioxide fixation as a central redox cofactor recycling mechanism in bacteria. *Proceedings of the National Academy of Sciences*, *107*(26), 11669–11675. https://doi.org/10.1073/pnas.1006175107

Meyer, J., Kelley, B. C., & Vignais, P. M. (1978). Effect of light on nitrogenase function and synthesis in *Rhodopseudomonas capsulata*. *Journal of Bacteriology*, *136*(1), 201–208.

Pereyra, D. S. V., & Ferrari, S. G. (2016). Extracellular Polymeric Substance (EPS) production by *Nostoc minutum* under different laboratory conditions. *Advances in Microbiology*, *6*(April), 374–380. https://doi.org/10.4236/aim.2016.65036

Pfennig, N. (1978). General Physiology and Ecology of Photosynthetic Bacteria. In R. K. Clayton & W. R. Sistrom (Eds.), *The Photosynthetic Bacteria* (pp. 3–18). New York: Plenum Press.

Puyol, D., Barry, E. M., Hülsen, T., & Batstone, D. J. (2017). A mechanistic model for anaerobic phototrophs in domestic wastewater applications: Photo-anaerobic model (PAnM). *Water Research*, *116*, 241–253. https://doi.org/10.1016/j.watres.2017.03.022

Reichert, P. (1994). AQUASIM – A tool for simulation and data analysis of aquatic systems. *Water Science and Technology*, *30*(2), 21–30. https://doi.org/10.2166/wst.1994.0025

Sasaki, K., Nishizawa, Y., & Nagai, S. (1980). Growth yield from electrons available from substrates in aerobic- and photoheterotrophic cultures of *Rhodopseudomonas sphaeroides* S. *Biotechnology and Bioengineering*, *22*(12), 2529–2541. https://doi.org/10.1002/bit.260221204

Schultz, J. E., & Weaver, P. F. (1982). Fermentation and Anaerobic Respiration by *Rhodospirillum rubrum* and *Rhodopseudomonas capsulata*. *Journal of Bacteriology*,

149(1), 181–190.

Siefert, E., Irgens, R. L., & Pfennig, N. (1978). Phototrophic purple and green bacteria in a sewage treatment plant. *Applied and Environmental Microbiology*, *35*(1), 38–44.

Sistrom, W. R. (1962). The kinetics of the synthesis of photopigments in *Rhodopseudomonas spheroides*. *Journal of General Microbiology*, *28*(4), 607–616. https://doi.org/10.1099/00221287-28-4-607

Sojka, G. A. (1978). Metabolism of nonaromatic organic compounds. In R. K. Clayton & W. R. Sistrom (Eds.), *The Photosynthetic BacteriaBacteria* (pp. 707–718). New York: Plenum Press.

Sojka, G. A., & Gest, H. (1968). Integration of energy conversion and biosynthesis in the photosynthetic bacterium *Rhodopseudomonas capsulata*. *Proceedings of the National Academy of Sciences*, *61*(4), 1486–1493. https://doi.org/10.1073/pnas.61.4.1486

Stevens, B. (2017). *Purple Phototropic Bacteria Enrichment, competition and bioproduct formation by purple non-sulfur photoheterotrophic bacteria in a mixed-culture sequencing batch reactor*. Delft University of Technology.

Tao, Y., He, Y., Wu, Y., Liu, F., Li, X., Zong, W., & Zhou, Z. (2008). Characteristics of a new photosynthetic bacterial strain for hydrogen production and its application in wastewater treatment. *International Journal of Hydrogen Energy*, *33*(3), 963–973. https://doi.org/10.1016/j.ijhydene.2007.11.021

Trabelsi, L., Ben Ouada, H., Bacha, H., & Ghoul, M. (2009). Combined effect of temperature and light intensity on growth and extracellular polymeric substance production by the cyanobacterium *Arthrospira platensis*. *Journal of Applied Phycology*, *21*(4), 405–412. https://doi.org/10.1007/s10811-008-9383-8

Uyar, B., Eroglu, I., Yücel, M., Gündüz, U., & Türker, L. (2007). Effect of light intensity, wavelength and illumination protocol on hydrogen production in photobioreactors. *International Journal of Hydrogen Energy*, *32*(18), 4670–4677. https://doi.org/10.1016/j.ijhydene.2007.07.002

van der Rest, M., & Gingras, G. (1974). The pigment complement of the photosynthetic center isolated from *Rhodospirillum rubrum**. *Journal of Biological Chemistry*, *249*(20), 6446–6453. Retrieved from http://www.jbc.org/content/249/20/6446.abstract

van Niel, C. B. (1944). The Culture, General Physiology, Morphology, and Classification of the Non-Sulfur Purple and Brown Bacteria. *Bacteriological Reviews*, *8*(1), 1–118. Retrieved from http://www.ncbi.nlm.nih.gov/pubmed/16350090%5Cnhttp://www.pubmedcentral.nih.go

v/articlerender.fcgi?artid=PMC440875

Vinet, L., & Zhedanov, A. (2011). A ‘missing’ family of classical orthogonal polynomials. *Journal of Physics A: Mathematical and Theoretical*, *44*(8), 085201. https://doi.org/10.1088/1751-8113/44/8/085201

Zürrer, H., & Bachofen, R. (1982). Aspects of growth and hydrogen production of the photosynthetic bacterium *Rhodospirillum rubrum* in continuous culture. *Biomass*, *2*(3), 165–174. https://doi.org/10.1016/0144-4565(82)90027-0

Appendix 1. Raw experimental data and calibration lines

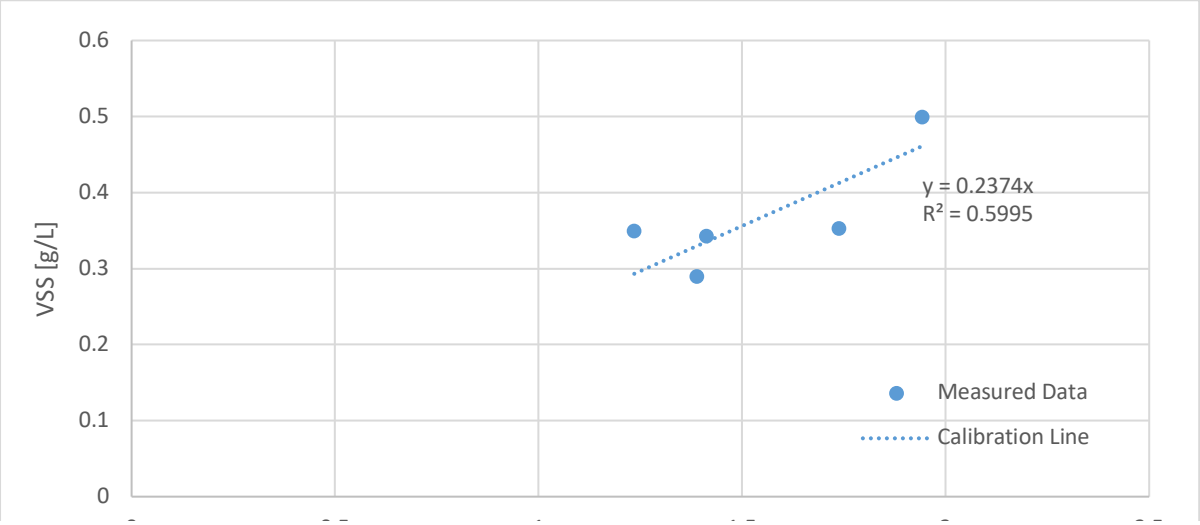

Figure 20. Calibration line of cell absorbance measured at 660 nm to VSS [g/L]. Dots are experimentally obtained data points and the dashed line is the calibration line. Each data point is not from a dilution series but from different time points.

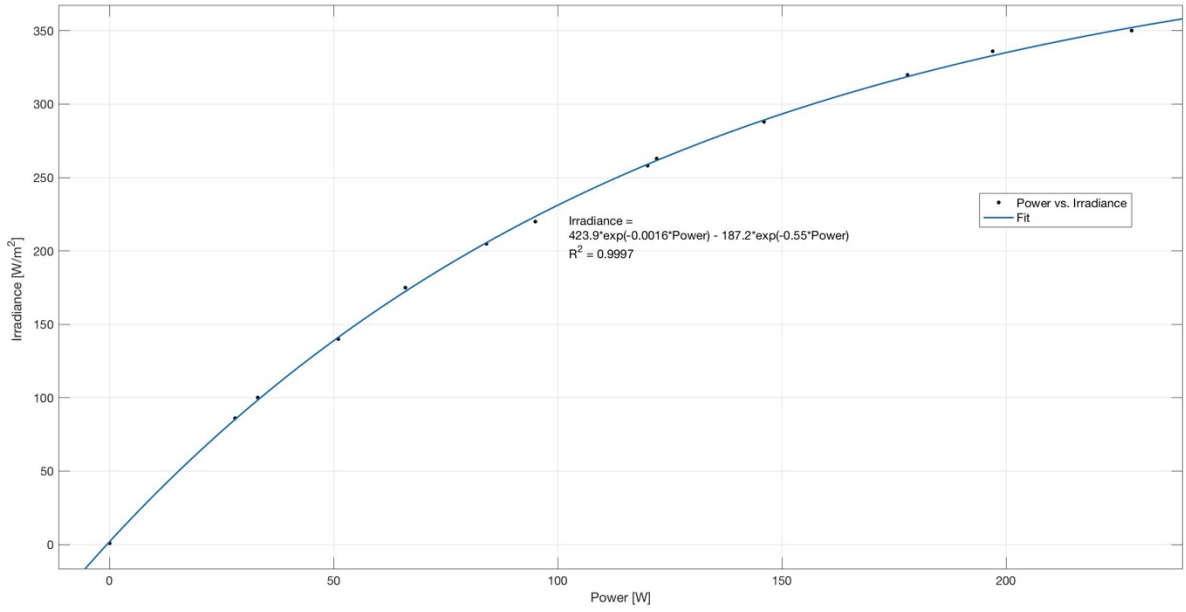

Figure 21. Calibration curve of power read by energy monitor versus measured irradiance by pyranomter. Energy consumption was monitored while measuring the irradiance read of pyranometer. It can be seen that the fitter curve is not linear but in an exponential form.

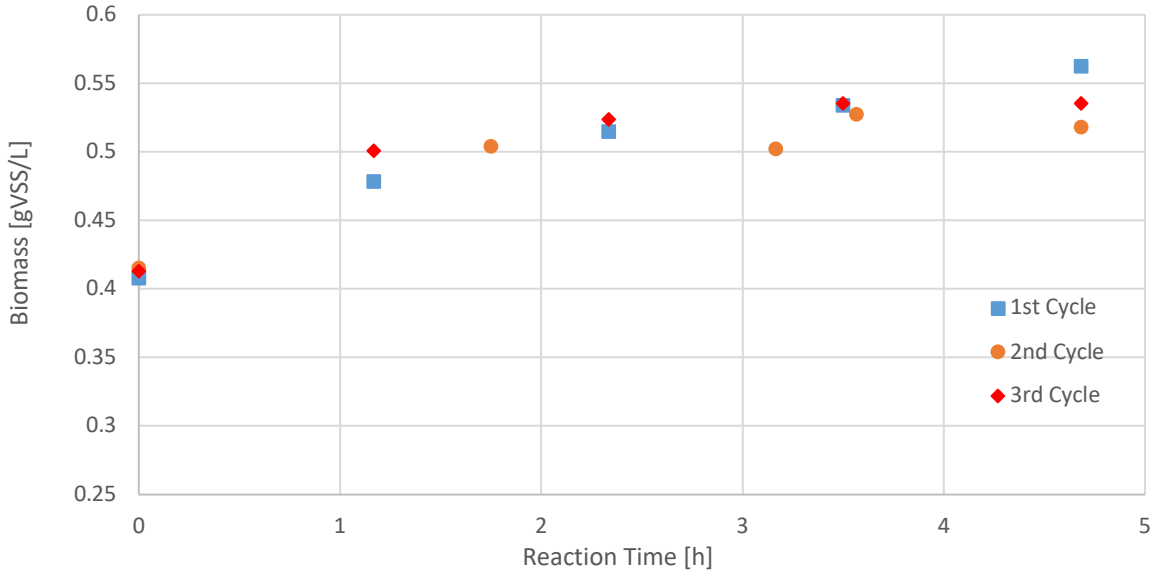

Figure 22. Biomass concentration change during reaction phase in baseline condition of 350W/m^2 incident light intensity. The three cycles in this figure come from three consecutive days of sampling, so there were 24 hours of

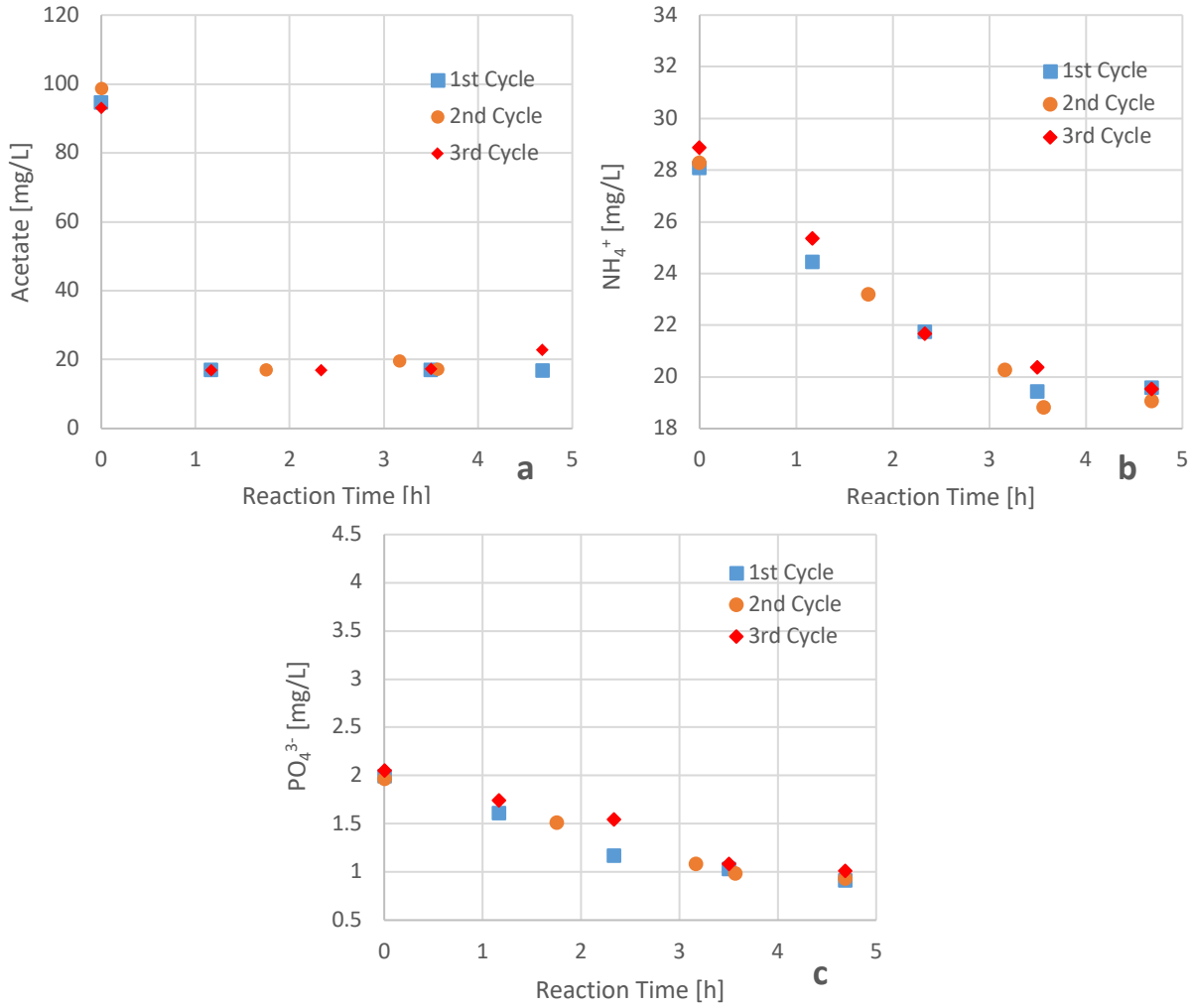

Figure 23. Substrate concentration change during reaction phase with baseline condition of 350W/m^2 of incident light intensity. **a** Acetate, **b** Ammonium, **c** Phosphate

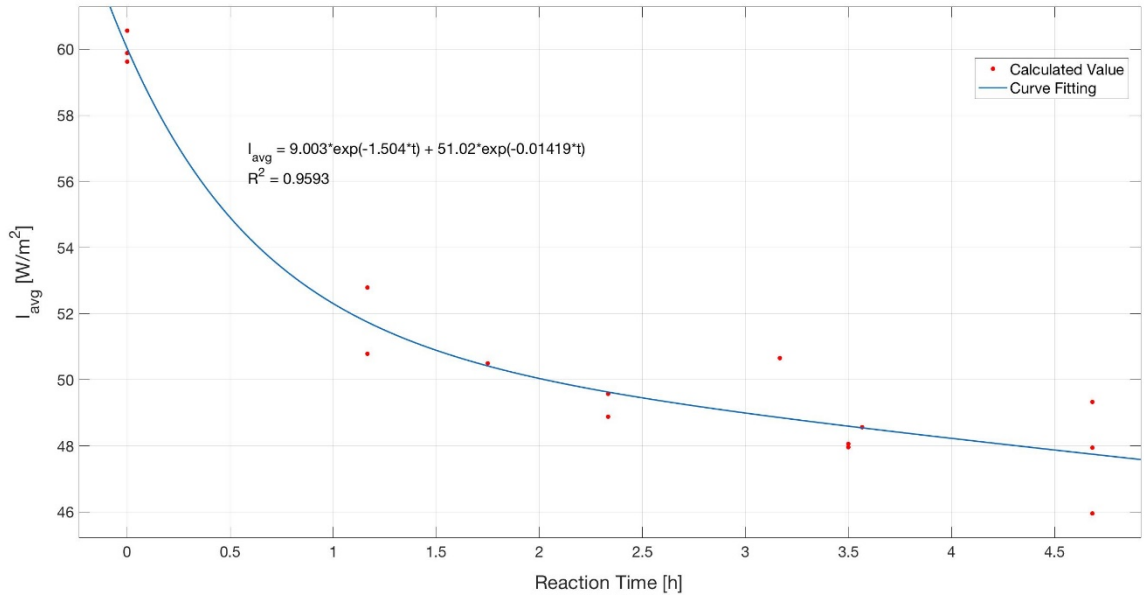

Figure 24. Average light intensity ($\boldsymbol{I_{avg}}$) change during the reaction phase with baseline incident light intensity (350W/m^2). Red dots are calculated $\boldsymbol{I_{avg}}$ values with experimentally obtained biomass concentration. Blue line is obtained by curve fitting of the red dots. Equation next to blue line is the fitted equation with the R^2 value.

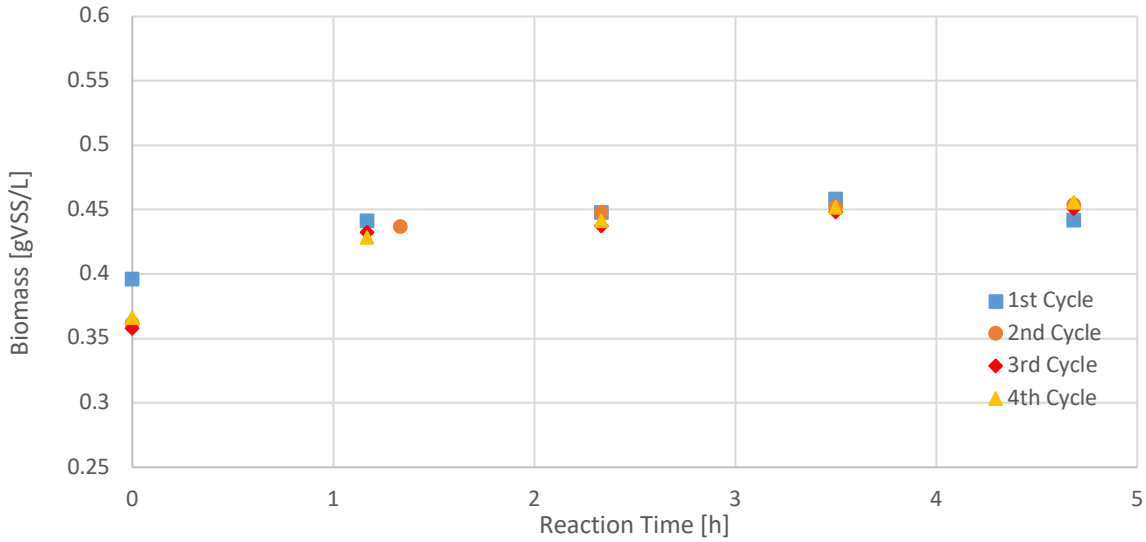

Figure 25. Biomass concentration change during reaction phase in 75% light condition of 262.5W/m^2 incident light intensity.

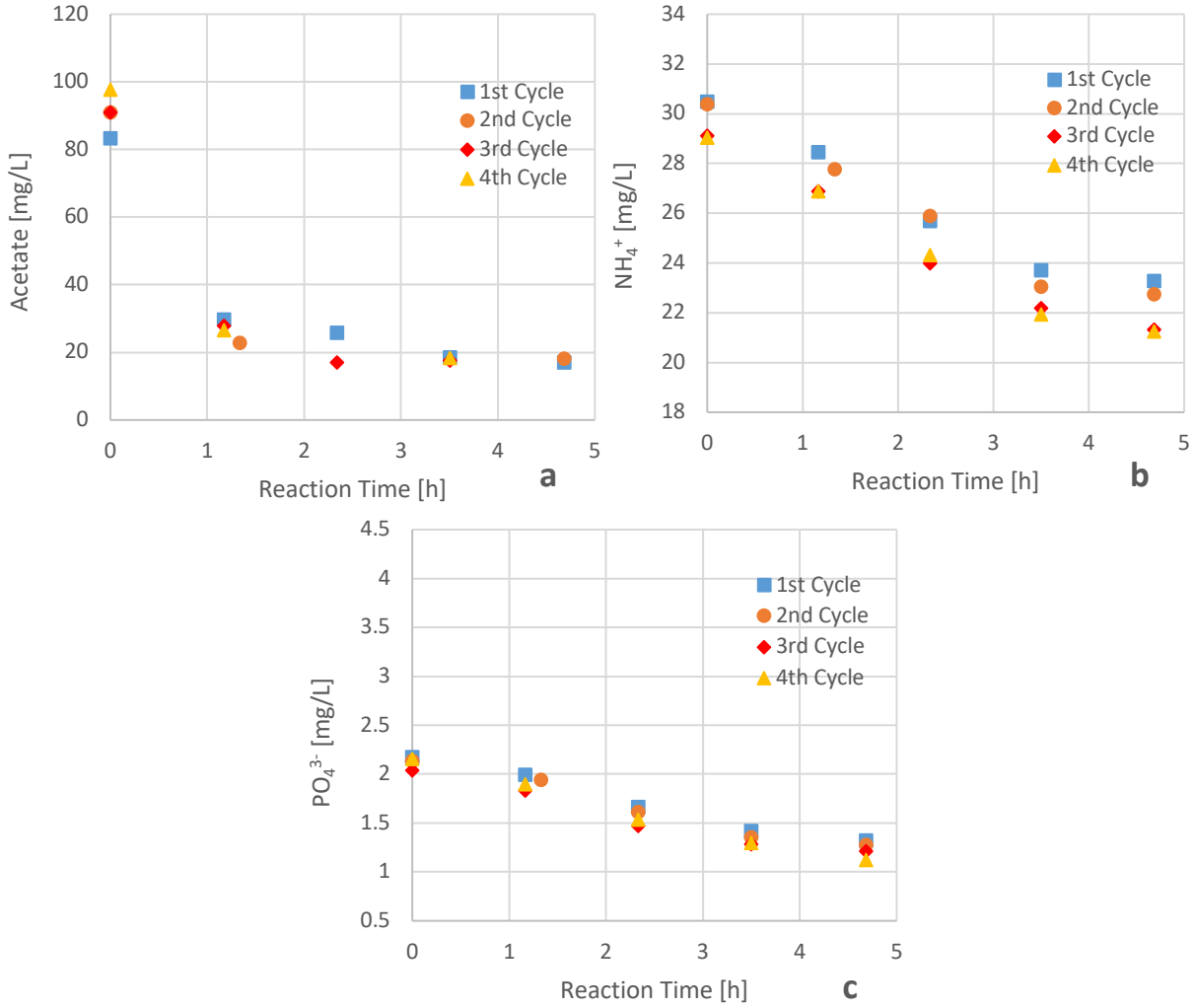

Figure 26. Substrate concentration change during reaction phase with 75% light condition of 262.5W/m^2 of incident light intensity. **a** Acetate, **b** Ammonium, **c** Phosphate

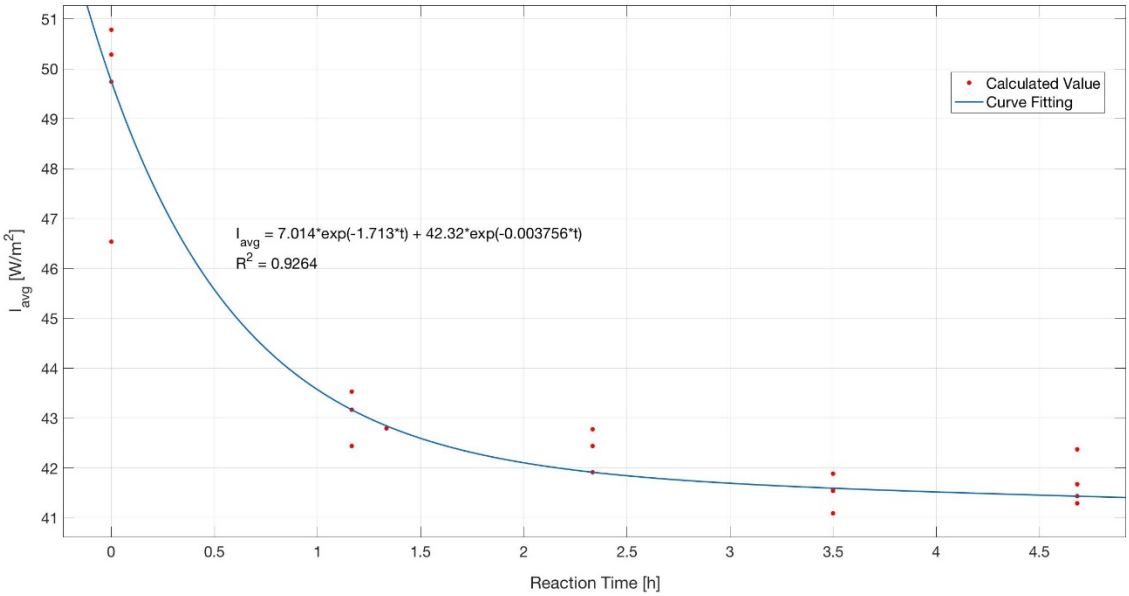

Figure 27. Average light intensity ($\boldsymbol{I_{avg}}$) change during the reaction phase with 75% of incident light intensity (262.5W/m^2). Red dots are calculated $\boldsymbol{I_{avg}}$ values with experimentally obtained biomass concentration. Blue line is obtained by curve fitting of the red dots. Equation next to blue line is the fitted equation with the R^2 value.

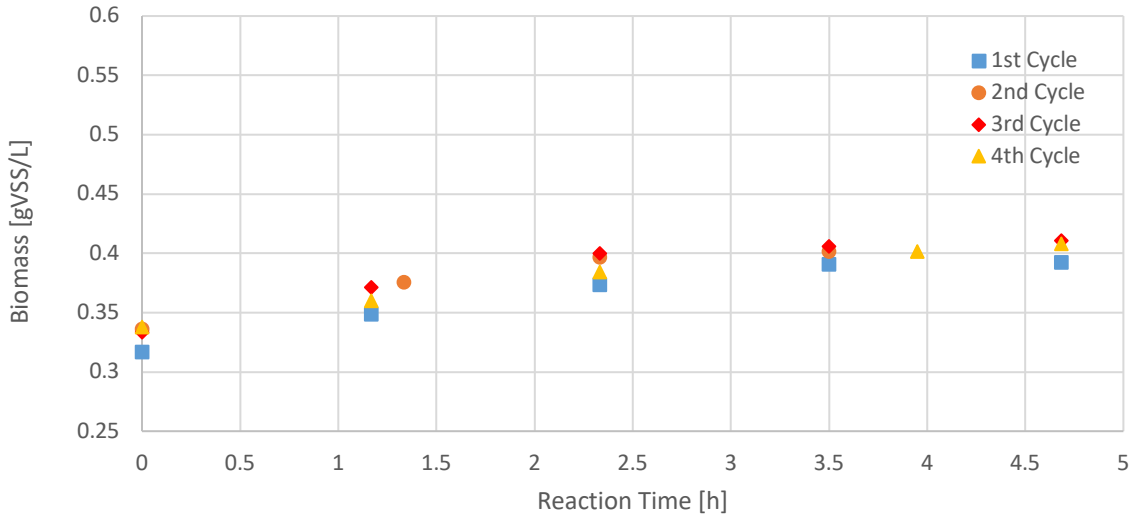

Figure 28. Biomass concentration change during reaction phase in 50% light condition of 175W/m^2 incident light intensity.

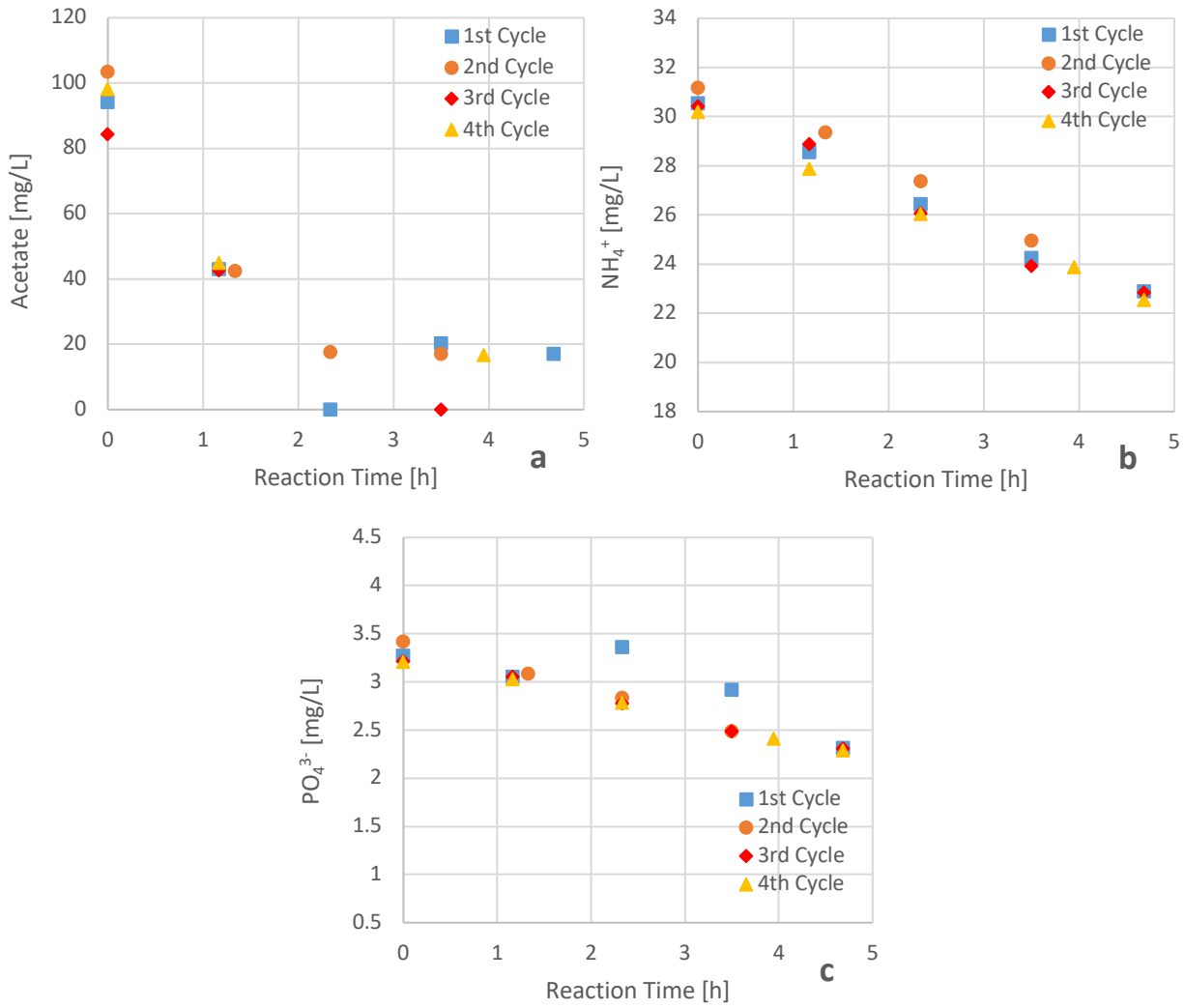

Figure 29. Substrate concentration change during reaction phase with 50% light condition of 262.5W/m^2 of incident light intensity. **a** Acetate, **b** Ammonium, **c** Phosphate

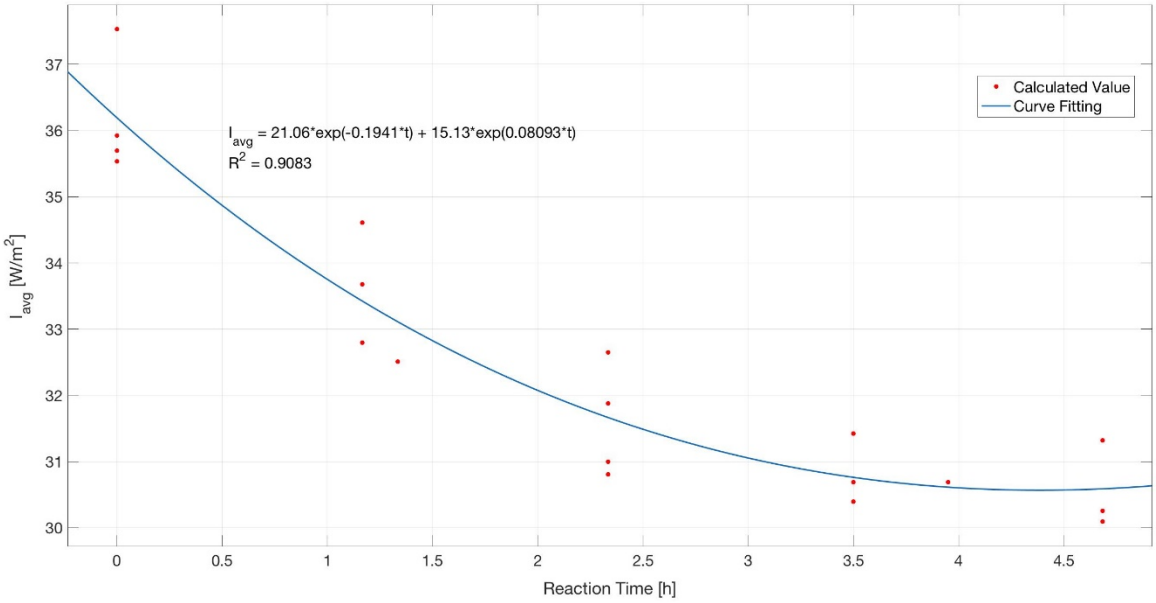

Figure 30. Average light intensity ($\boldsymbol{I_{avg}}$) change during the reaction phase with 50% of incident light intensity (175W/m^2). Red dots are calculated $\boldsymbol{I_{avg}}$ values with experimentally obtained biomass concentration. Blue line is obtained by curve fitting of the red dots. Equation next to blue line is the fitted equation with the R^2 value.

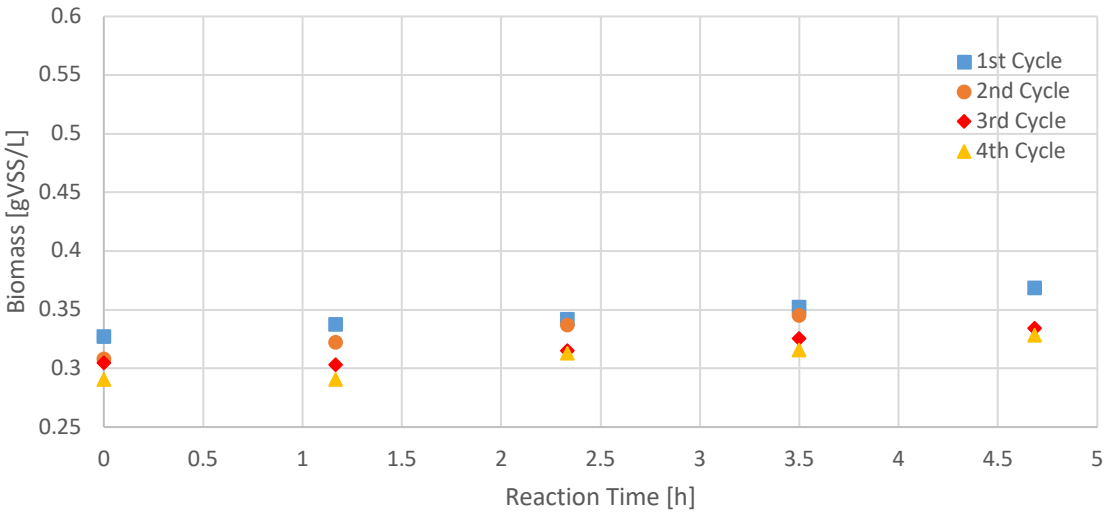

Figure 31. Biomass concentration change during reaction phase in 25% light condition of 87.5W/m^2 incident light intensity.

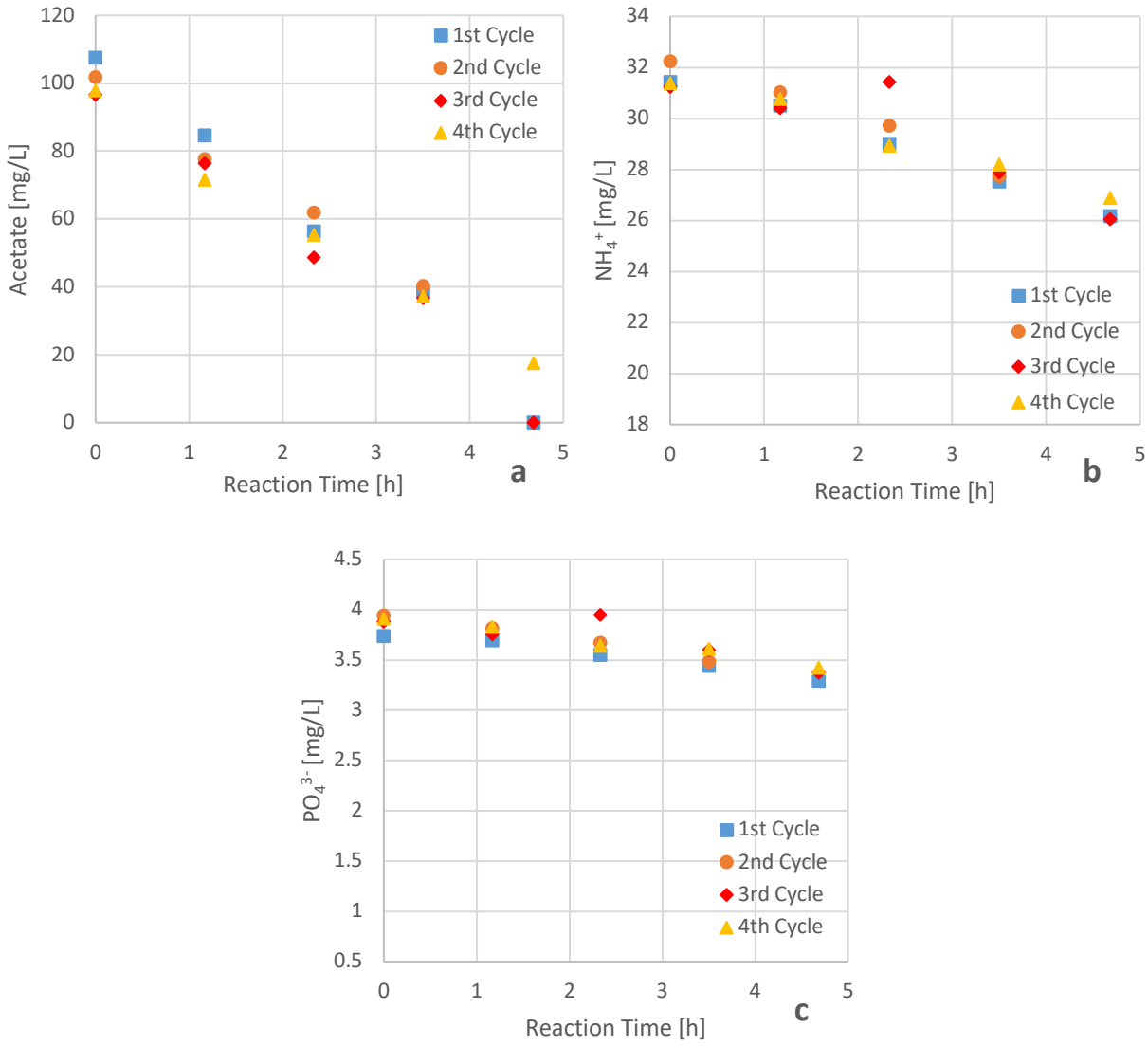

Figure 32. Substrate concentration change during reaction phase with 25% light condition of 87.5W/m^2 of incident light intensity. **a** Acetate, **b** Ammonium, **c** Phosphate

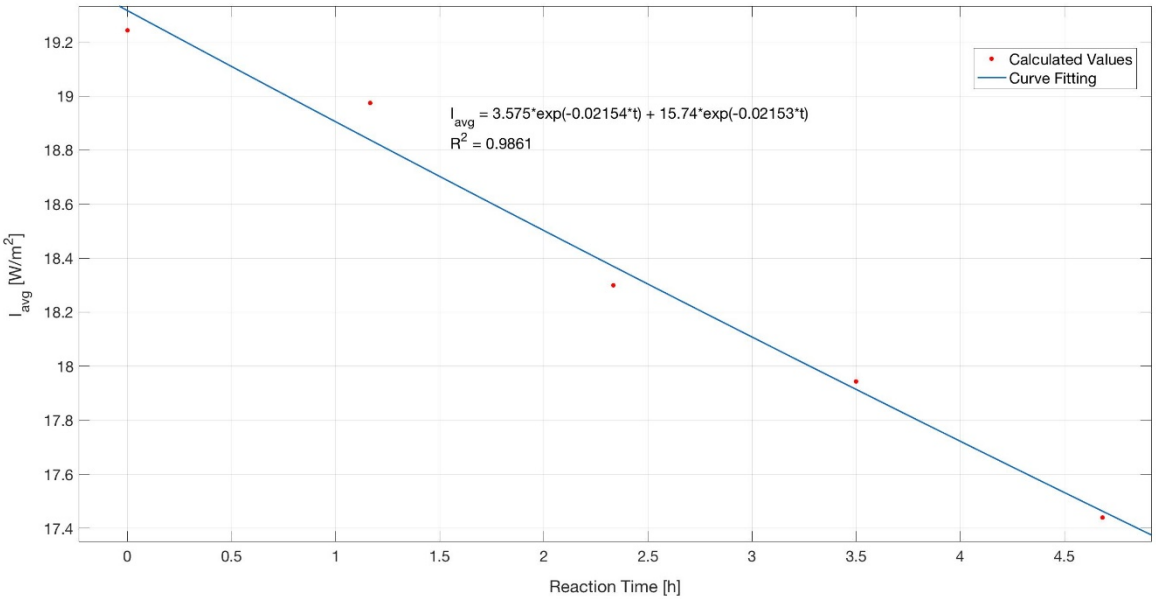

Figure 33. Average light intensity ($\boldsymbol{I_{avg}}$) change during the reaction phase with 25% of incident light intensity (87.5W/m^2). Unlike the previous three settings, in 25% intensity, due to large fluctuation in biomass concentration, the $\boldsymbol{I_{avg}}$ was calculated for average biomass concentration. Red dots are calculated $\boldsymbol{I_{avg}}$ values with experimentally obtained biomass concentration. Blue line is obtained by curve fitting of the red dots. Equation next to blue line is the fitted equation with the R^2 value.

Table 4. Bacteriochlorophyll content in different light settings with their average absorbance value at different points of measurement.

	Baseline		**75% Light**		**50% Light**		**25% Light**	
	Absorbance*	Content** [mg BChl /mg VSS]	Absorbance*	Content** [mg BChl /mg VSS]	Absorbance*	Content** [mg BChl /mg VSS]	Absorbance*	Content** [mg BChl /g VSS]
1st Cycle	0.442 (start) 0.402 (2nd) 0.464 (3rd) 0.4525 (4th) 0.458 (end)	21.2 (3.0)	0.428 (start) 0.4525 (2nd) 0.3675 (3rd) 0.384 (4th) 0.3935 (end)	27.4 (3.1)	0.281 (start) 0.274 (2nd) 0.288 (3rd) 0.288 (4th) 0.3285 (end)	20.1 (1.9)	0.2575 (start) 0.2465 (2nd) 0.2585 (3rd) 0.2765 (4th) 0.2805 (end)	18.7 (0.7)
2nd Cycle	0.4325 (start) 0.384 (2nd) 0.394 (3rd) 0.417 (4th) 0.4505 (end)	20.8 (3.3)	0.445 (start) 0.332 (2nd) 0.3535 (3rd) 0.323 (4th) 0.389 (end)	25.5 (4.9)	0.3095 (start) 0.274 (2nd) 0.2955 (3rd) 0.2975 (4th) - (end)	19.6 (2.7)	0.23 (start) 0.244 (2nd) 0.248 (3rd) 0.2665 (4th) 0.265 (end)	18.4(0.4)
3rd Cycle	0.393 (start) 0.3945 (2nd) 0.4 (3rd) 0.4035 (4th) 0.421 (end)	19.8 (2.4)	0.2935 (start) 0.2905 (2nd) 0.294 (3rd) 0.3015 (4th) 0.3335 (end)	21.0 (1.0)	0.287 (start) 0.314 (2nd) 0.281 (3rd) 0.291 (4th) 0.2975 (end)	19.3 (2.0)	0.2125 (start) 0.2235 (2nd) 0.2375 (3rd) 0.2375 (4th) 0.2245 (end)	17.6 (0.6)
4th Cycle	-		0.3015 (start) 0.318 (2nd) 0.3285 (3rd) - (4th) 0.3485 (end)	22.4 (0.8)	0.283 (start) 0.317 (2nd) 0.2645 (3rd) 0.2925 (4th) 0.2935 (end)	19.3 (2.1)	0.1955 (start) 0.208 (2nd) 0.2205 (3rd) 0.2235 (4th) 0.2245 (end)	17.1 (0.2)
Setting Average	-	20.6 (0.7)	-	24.1 (2.9)	-	19.6 (0.4)	-	18.0 (0.7)

* Order inside brackets under absorbance column stands for time order of sampling within each cycle
** Values inside brackets under the content column stands for standard deviation.

Appendix 2. Growth simulation in Aquasim

```
*******************************************************************************

AQUASIM Version 2.1g (win/mfc) - Listing of System Definition

*******************************************************************************

Date and time of listing:  10/07/2018  16:02:09

*******************************************************************************
Variables
*******************************************************************************
alpha:          Description:          Ratio of biomass loss after settlin
                                      g phase
                Type:                 Constant Variable
                Unit:
                Value:                0.01
                Standard Deviation:   1
                Minimum:              0
                Maximum:              10
                Sensitivity Analysis: inactive
                Parameter Estimation: inactive
-------------------------------------------------------------------------------
Exp_S_ac_1:     Description:          Experimentally obtained acetate con
                                      centration set 1
                Type:                 Real List Variable
                Unit:
                Argument:             t
                Standard Deviations:  global
                Rel. Stand. Deviat.:  0
                Abs. Stand. Deviat.:  1
                Minimum:              0
                Maximum:              1e+009
                Interpolation Method: linear interpolation
                Sensitivity Analysis: inactive
                Real Data Pairs (4 pairs):
                   115.25          94.6788
                   116.416         16.9942
                   118.75          16.9942
                   119.9333        16.9341
```

```
--------------------------------------------------------------------------
Exp_S_ac_2:    Description:          Experimentally obtained acetate con
                                     centration set 2
               Type:                 Real List Variable
               Unit:
               Argument:             t
               Standard Deviations:  global
               Rel. Stand. Deviat.:  0
               Abs. Stand. Deviat.:  1
               Minimum:              0
               Maximum:              1e+009
               Interpolation Method: linear interpolation
               Sensitivity Analysis: inactive
               Real Data Pairs (4 pairs):
                  115.25          98.78225
                  117             17.1743
                  118.416         19.6964
                  119.166         17.4145
--------------------------------------------------------------------------
Exp_S_ac_3:    Description:          Experimentally obtained acetate con
                                     centration set 3
               Type:                 Real List Variable
               Unit:
               Argument:             t
               Standard Deviations:  global
               Rel. Stand. Deviat.:  0
               Abs. Stand. Deviat.:  1
               Minimum:              0
               Maximum:              1e+009
               Interpolation Method: linear interpolation
               Sensitivity Analysis: inactive
               Real Data Pairs (5 pairs):
                  115.25          93.037467
                  116.416         16.87405
                  117.583         16.87405
                  118.75          17.35445
                  119.9333        22.819
--------------------------------------------------------------------------
Exp_S_am_1:    Description:          Experimentally obtained ammonium co
                                     ncentration set 1
               Type:                 Real List Variable
```

```
                Unit:
                Argument:             t
                Standard Deviations:  global
                Rel. Stand. Deviat.:  0
                Abs. Stand. Deviat.:  1
                Minimum:              0
                Maximum:              1e+009
                Interpolation Method: linear interpolation
                Sensitivity Analysis: inactive
                Real Data Pairs (5 pairs):
                   115.25          28.098
                   116.416         24.4445
                   117.583         21.75703
                   118.75          19.435715
                   119.9333        19.59983
--------------------------------------------------------------------------
Exp_S_am_2:     Description:          Experimentally obtained ammonium co
                                      ncentration set 2
                Type:                 Real List Variable
                Unit:
                Argument:             t
                Standard Deviations:  global
                Rel. Stand. Deviat.:  0
                Abs. Stand. Deviat.:  1
                Minimum:              0
                Maximum:              1e+009
                Interpolation Method: linear interpolation
                Sensitivity Analysis: inactive
                Real Data Pairs (5 pairs):
                   115.25          28.29339
                   117             23.192355
                   118.416         20.28618
                   119.166         18.830395
                   119.9333        19.0701
--------------------------------------------------------------------------
Exp_S_am_3:     Description:          Experimentally obtained ammonium co
                                      ncentration set 3
                Type:                 Real List Variable
                Unit:
                Argument:             t
                Standard Deviations:  global
```

```
                Rel. Stand. Deviat.:  0
                Abs. Stand. Deviat.:  1
                Minimum:              0
                Maximum:              1e+009
                Interpolation Method: linear interpolation
                Sensitivity Analysis: inactive
                Real Data Pairs (5 pairs):
                   115.25          28.88244
                   116.416         25.37321
                   117.583         21.666305
                   118.75          20.37426
                   119.9333        19.543735
------------------------------------------------------------------------
Exp_X_p_1:      Description:          Experimentally obtained biomass con
                                      centration set 1
                Type:                 Real List Variable
                Unit:
                Argument:             t
                Standard Deviations:  global
                Rel. Stand. Deviat.:  0
                Abs. Stand. Deviat.:  1
                Minimum:              0
                Maximum:              1e+009
                Interpolation Method: linear interpolation
                Sensitivity Analysis: inactive
                Real Data Pairs (5 pairs):
                   115.25          407.8532
                   116.416         478.5984
                   117.583         514.9206
                   118.75          533.9126
                   119.9333        562.2819
------------------------------------------------------------------------
Exp_X_p_2:      Description:          Experimentally obtained biomass con
                                      centration set 2
                Type:                 Real List Variable
                Unit:
                Argument:             t
                Standard Deviations:  global
                Rel. Stand. Deviat.:  0
                Abs. Stand. Deviat.:  1
                Minimum:              0
```

```
                Maximum:              1e+009
                Interpolation Method: linear interpolation
                Sensitivity Analysis: inactive
                Real Data Pairs (5 pairs):
                   115.25          415.3313
                   117             504.1189
                   118.416         502.2197
                   119.166         527.3841
                   119.9333        517.888
-------------------------------------------------------------------------
Exp_X_p_3:      Description:          Experimentally obtained biomass con
                                      centration set 3
                Type:                 Real List Variable
                Unit:
                Argument:             t
                Standard Deviations:  global
                Rel. Stand. Deviat.:  0
                Abs. Stand. Deviat.:  1
                Minimum:              0
                Maximum:              1e+009
                Interpolation Method: linear interpolation
                Sensitivity Analysis: inactive
                Real Data Pairs (5 pairs):
                   115.25          413.1947
                   116.416         500.7953
                   117.583         523.467
                   118.75          535.2183
                   119.9333        535.4557
-------------------------------------------------------------------------
F_ac_in:        Description:          Acetate dosing
                Type:                 Formula Variable
                Unit:                 mg/h
                Expression:           Qin*S_ac_in
-------------------------------------------------------------------------
F_am_in:        Description:          Ammonium dosing
                Type:                 Formula Variable
                Unit:                 mg/h
                Expression:           Qin*S_am_in
-------------------------------------------------------------------------
K_ac:           Description:          Half velocity constant of acetate (
                                      empirically chosen)
```

	Type:	Constant Variable
	Unit:	mg/L
	Value:	0.5
	Standard Deviation:	1
	Minimum:	0
	Maximum:	50
	Sensitivity Analysis:	active
	Parameter Estimation:	active

K_am:	Description:	Half velocity constant of ammonium (empirically chosen)
	Type:	Constant Variable
	Unit:	mg/L
	Value:	2
	Standard Deviation:	1
	Minimum:	0
	Maximum:	30
	Sensitivity Analysis:	active
	Parameter Estimation:	active

K_I:	Description:	Half velocity of Irradiance (empirically chosen)
	Type:	Constant Variable
	Unit:	W/m2
	Value:	20
	Standard Deviation:	1
	Minimum:	0
	Maximum:	100
	Sensitivity Analysis:	active
	Parameter Estimation:	active

---

mu_max:	Description:	Maximum specific growth rate
	Type:	Formula Variable
	Unit:	1/h
	Expression:	0.0825

---

m_X:	Description:	Total biomass
	Type:	Formula Variable
	Unit:	mg
	Expression:	X∗V

```
Q:              Description:          Discharge
                Type:                 Program Variable
                Unit:                 L/h
                Reference to:         Discharge
------------------------------------------------------------------------
Qeff:           Description:          Effluent flow rate (Scheduled)
                Type:                 Real List Variable
                Unit:                 L/h
                Argument:             t_fract
                Standard Deviations:  global
                Rel. Stand. Deviat.:  0
                Abs. Stand. Deviat.:  1
                Minimum:              0
                Maximum:              1e+009
                Interpolation Method: linear interpolation
                Sensitivity Analysis: inactive
                Real Data Pairs (6 pairs):
                   0              0
                   3              0
                   3.0001         8.88
                   3.0833         8.88
                   3.0834         0
                   8              0
------------------------------------------------------------------------
Qin:            Description:          Inflow rate (Scheduled)
                Type:                 Real List Variable
                Unit:                 L/h
                Argument:             t_fract
                Standard Deviations:  global
                Rel. Stand. Deviat.:  0
                Abs. Stand. Deviat.:  1
                Minimum:              0
                Maximum:              1e+009
                Interpolation Method: linear interpolation
                Sensitivity Analysis: inactive
                Real Data Pairs (6 pairs):
                   0              0
                   3.1666         0
                   3.1667         12.6
                   3.2499         12.6
                   3.25           0
```

```
                  8               0
-------------------------------------------------------------------------
Qp:               Description:          Purge flow (Scheduled)
                  Type:                 Real List Variable
                  Unit:                 L/h
                  Argument:             t_fract
                  Standard Deviations:  global
                  Rel. Stand. Deviat.:  0
                  Abs. Stand. Deviat.:  1
                  Minimum:              0
                  Maximum:              1e+009
                  Interpolation Method: linear interpolation
                  Sensitivity Analysis: inactive
                  Real Data Pairs (5 pairs):
                     0                  0
                     7.9333             0
                     7.9334             4.65
                     7.9999             4.65
                     8                  0
-------------------------------------------------------------------------
S_ac:             Description:          Acetate concentration in reactor
                  Type:                 Dyn. Volume State Var.
                  Unit:                 mg/L
                  Relative Accuracy:    1e-006
                  Absolute Accuracy:    1e-006
-------------------------------------------------------------------------
S_ac_in:          Description:          Inflow acetate concentration
                  Type:                 Constant Variable
                  Unit:                 mg/L
                  Value:                218
                  Standard Deviation:   1
                  Minimum:              0
                  Maximum:              300
                  Sensitivity Analysis: inactive
                  Parameter Estimation: inactive
-------------------------------------------------------------------------
S_am:             Description:          Ammonium concentration in reactor
                  Type:                 Dyn. Volume State Var.
                  Unit:                 mg/L
                  Relative Accuracy:    1e-006
                  Absolute Accuracy:    1e-006
```

```
--------------------------------------------------------------------------
S_am_in:       Description:          Inflow ammonium concentration
               Type:                 Constant Variable
               Unit:                 mg/L
               Value:                38.62
               Standard Deviation:   1
               Minimum:              0
               Maximum:              100
               Sensitivity Analysis: inactive
               Parameter Estimation: inactive
--------------------------------------------------------------------------
S_I:           Description:          Available Light
               Type:                 Formula Variable
               Unit:                 W/m2
               Expression:           181.9*exp(-0.007049*X)+78.45*exp(-0
                                     .00109*X)
--------------------------------------------------------------------------
t:             Description:          Time
               Type:                 Program Variable
               Unit:                 h
               Reference to:         Time
--------------------------------------------------------------------------
t_fract:       Description:          Fractionation of time with 8 hours
               Type:                 Formula Variable
               Unit:                 h
               Expression:           t mod 8
--------------------------------------------------------------------------
V:             Description:          Reactor Volume (Bulk)
               Type:                 Program Variable
               Unit:                 L
               Reference to:         Reactor Volume
--------------------------------------------------------------------------
X:             Description:          Biomass concentration
               Type:                 Dyn. Volume State Var.
               Unit:                 mg/L
               Relative Accuracy:    1e-006
               Absolute Accuracy:    1e-006
--------------------------------------------------------------------------
Y_xac:         Description:          Biomass yield on Acetate
               Type:                 Formula Variable
               Unit:                 mgX/mgAc
```

```
              Expression:           0.675
--------------------------------------------------------------------------
Y_xam:        Description:          Biomass yield on Ammonium
              Type:                 Formula Variable
              Unit:                 mgX/mgAm
              Expression:           6.91
**************************************************************************

**************************************************************************
Processes
**************************************************************************
PNSB_growth:  Description:          PNSB growth on Acetate as C-source
                                    and Ammonium as N-source
              Type:                 Dynamic Process
              Rate:                 (mu_max*S_ac/(K_ac+S_ac)*S_am/(K_am
                                    +S_am)*S_I/(S_I+K_I))*X
              Stoichiometry:
                Variable : Stoichiometric Coefficient
                X : 1
                S_ac : -1/Y_xac
                S_am : -1/Y_xam
**************************************************************************

**************************************************************************
Compartments
**************************************************************************
Discharge_Tank:Description:         Discharge collection tank needed fo
                                    r settling phase imitation for SBR
                                    operation
              Type:                 Mixed Reactor Compartment
              Compartment Index:    0
              Active Variables:
              Active Processes:
              Initial Conditions:
              Inflow:               0
              Loadings:
              Volume:               1
              Accuracies:
                Rel. Acc. Q:        0.001
```

```
                Abs. Acc. Q:        0.001
                Rel. Acc. V:        0.001
                Abs. Acc. V:        0.001
--------------------------------------------------------------------------
SBR_4:          Description:        Sequencing Batch Reactor on operati
                                    on 4 mode
                Type:               Mixed Reactor Compartment
                Compartment Index:  0
                Active Variables:   X, S_ac, S_am
                Active Processes:   PNSB_growth
                Initial Conditions:
                  Variable(Zone) : Initial Condition
                  X(Bulk Volume) : 480
                  V(Bulk Volume) : 1.79
                  S_ac(Bulk Volume) : 18
                  S_am(Bulk Volume) : 22
                Inflow:             Qin
                Loadings:
                  Variable : Loading
                  S_ac : F_ac_in
                  S_am : F_am_in
                Outflow:            Qeff+Qp
                Accuracies:
                  Rel. Acc. Q:      0.001
                  Abs. Acc. Q:      0.001
                  Rel. Acc. V:      0.001
                  Abs. Acc. V:      0.001
**************************************************************************


**************************************************************************
Links
**************************************************************************
link1:          Description:        Link from SBR_4 to comp2 for supern
                                    atant withdrawal imitation
                Type:               Advective Link
                Link Index:         0
                Compartment In:     SBR_4
                Connection In:      Outflow
                Compartment Out:    Discharge_Tank
                Connection Out:     Inflow
```

```
               Bifurcations:
                 Settling:
                   Description:Trick to imitate settling phase of SBR
                   Compartment Out:  SBR_4
                   Connection Out:   Inflow
                   Water Flow:       0
                   Mass Loadings:
                     Variable : Loading
                     X : (1-alpha)*X*Qeff
-------------------------------------------------------------------------
link2:         Description:          Discharge of supernatant coming fro
                                     m SBR_4
               Type:                 Advective Link
               Link Index:           0
               Compartment In:       Discharge_Tank
               Connection In:        Outflow
               Compartment Out:
               Bifurcations:
*************************************************************************


*************************************************************************
Definitions of Calculations
*************************************************************************
calc1:         Description:
               Calculation Number:   0
               Initial Time:         0
               Initial State:        given, made consistent
               Step Size:            0.0005
               Num. Steps:           240000
               Status:               active for simulation
                                     active for sensitivity analysis
*************************************************************************


*************************************************************************
Calculation Parameters
*************************************************************************
Numerical Parameters:    Maximum Int. Step Size:  0.001
                         Maximum Integrat. Order: 5
                         Number of Codiagonals:   1000
```

```
                        Maximum Number of Steps: 10000000
------------------------------------------------------------------------------
                        Fit Method:              secant
                        Max. Number of Iterat.:  10000
******************************************************************************
```

Appendix 3. Light distribution model in Matlab

```
%%% Calculation of light intensity profile in cylindrical reactor

% Substances/Materials to consider are a)medium, b)PNSB and c)photoreactor.
% For simplicity, light is uniformly provided in horizontal direction and
% its intensity does not change in vertical direction. Also the reactor
% is assumed to be ideally mixed and no biofilm accumulation at the wall of
% the reactor is occurring. Moreover, the glass wall of the reactor does
% not have any light attenuation effect. The reactor is cylindrical shaped
% so the light intensity inside the reactor is a function of distance from
% the center of the reactor. Medium does not attenuate any light in the
% wavelength range of 290 nm to 999 nm.

% I = f(r,X_p): Light attenuation equation adapted from Katsuda et al. 2000
% and Katsuda et al. 2002 with some modification to match with the reactor
% characteristics.

tic
lambda = 290:1:999;             % Wavelength [nm]
I_0 = 350;                      % Incident light intensity measured at the surface of
the reactor [W/m^2]
I_0l = I_0/length(lambda);      % Assume uniform spectral irradiance [W/m^2/nm]
L_0 = 0.20;                     % Distance to surface of reactor from light source [m]
filename = 'Extinction Coefficient.xlsx';% Extinction coefficient of cell [m^2/g]
e_cell = xlsread(filename);
e_cell = e_cell(:,2)';
R = 0.065;                      % Radius of the reactor [m]
r=[0:1:R*1000]./1000;           % Distance from wall surface of reactor [m]
X_p = X_p.*1000;                % Biomass concentration unit conversion [g/m^3]


% Due to the size of data, it is unavailable to store them in a single ordinary
% array. Thus, they are evenly divided into smaller matrices and stored in
% a cell array. In the final step, each elements are stacked to return an
% ordinary array (2D matrix).

P{n,1} = [];                    % Preallocate to reduce calculation time

for j = 1:n
    for i = 1:length(r)
        P{j,1}(1:length(X_p)/n,:,i) = I_0l.*((L_0^2./(L_0+r(i)).^2).*10.^(X_p(1+(j-
1)*length(X_p)/n:length(X_p)/n*j)'.*(-e_cell).*(r(i)))...
            +(L_0^2./(L_0+2*R-r(i)).^2).*10.^(X_p(1+(j-
1)*length(X_p)/n:length(X_p)/n*j)'.*(-e_cell).*(2*R-r(i))));
    end
end

for j = 1:n
    P{j,1} = sum(P{j,1},2);     % Sum with respect to wavelength
    P{j,1} = reshape(P{j,1}, [length(X_p)/n length(r)]);    % Reshape 3D matrix to 2D
matrix
end

I_l = cell2mat(P);              % Stacking all elements to return an ordinary array

figure
surf(X_p,r,I_l','edgecolor', 'none');
xlabel('Biomass Concentration (X_p) [g/m^3]', 'FontSize', 14);
ylabel('Distance (r) [m]','FontSize', 14);
zlabel('Irradiance (I) [W/m^2]','FontSize', 14);
title('Biomass concentration vs Distance vs Irradiance','FontSize', 18)
```

```
figure
plot(X_p,I_l(:,1));
xlabel('Biomass Concentration (X_p) [g/m^3]', 'FontSize', 14);
ylabel('Irradiance (I) [W/m^2]','FontSize', 14);
title('Biomass concentration vs Irradiance at Center of Reactor','FontSize', 18)

toc
```